The Viability of Black Locust and the Triakonta Connection System as Structural Components in Modular Framing Systems

Russell B. Womer

January 2012

Abstract

Modern building structural materials, such as concrete and steel, embody relatively high amounts of energy and detrimentally contribute to the building industry's high output of greenhouse gases. Additionally, semi-permanent modern building construction methods used with these materials, such as welding and wet work detrimentally contribute to the building industry's large contribution of landfill wastes. In response to these two issues, Professor Jack Elliott of Cornell University has developed a new structural system known as "Triakonta", a modular wood-based, carbon-sequestering system designed for disassembly, to reduce landfill wastes. The purpose of this thesis research is to investigate the structural viability of the Triakonta framing system, utilizing black locust timber as the carbon sequestering material in conjunction with a novel modular connector system. Through a proof of concept prototyping effort, and a mechanical testing program, the assembly's basic mechanical characteristics under loading, and its viability as a complete structural system were tested. Quarter scale modeling and full scale mechanical testing in tension, compression, and bending were undertaken at the Bovay Civil Infrastructure Laboratory Complex at Cornell University. The results from these prototype trials demonstrate the viability of the system as a flexible, environmentally conscious alternative to conventional construction.

Biographical Sketch

Russell Womer graduated in 2009 from Cornell University with a degree in Design and Environmental Analysis (DEA) with a focus on Facilities Planning and Management. Furthering his interests in sustainable and environmentally conscious environmental design, Russell enrolled in the newly created Master's program in Sustainable Design Studies at Cornell that fall.

Since the summer of 2010 Russell has lived in North Carolina pursuing his career as a Product Manager for the software company FM:Systems, developing software used in the management and planning of facilities and real estate and honing his interests in workplace strategy, environmentally conscious facilities practice, and high performance building design. In addition to his continuing studies and career responsibilities, Russell has begun writing periodically for the Facilities Management Journal (FMJ) on topics related to the sustainable workplace, and working with the IFMA Foundation on the production of industry publications.

Acknowledgements

First, I would like to thank all of the Faculty and Staff who helped me both with their time and experience in bringing this project to completion. I would like to thank George Petry, Chief technician at the Emerson Lab, for his instruction and council on the development and fabrication of the system. I would like to thank Timothy Bond, chief supervisor of the Bovay Civil Infrastructure Laboratory Complex at Cornell University, whose guidance and experience lead the testing of the system prototypes and made this research possible. I would like to thank Tony Ingraffea, the Dwight C. Baum Professor of Engineering at the Cornell University School of Civil Engineering, for his tutelage and patience in the area of structural mechanics and materials science, without which I would have been lost. I would also like to thank those outside of Cornell who donated their time, and resources to help realize this project, including Gordon Cowley, who donated his time to tour his facility and learn about his work and Tom Brown, who generously donated the Black Locust material for use in the system. I would like to include a special thank you to all of my classmates who assisted Jack and I on the production of the Triakonta system. Lastly, this paper is dedicated to my Professor and friend Jack Elliott, whose patience and dedication to my own learning helped me to discover a more complete and meaningful understanding of design, the built environment, and our environmental and social responsibilities therein.

Table of Contents

Contents

Abstract 3

Biographical Sketch 3

Acknowledgements 4

Table of Contents 5

Tables and Figures: 7

Introduction 8

Background (Literature Review) 10

- The Problem with Carbon 10
- Wood as an Engineered Material 14
- Black Locust 15
- The Evolution of Connection Technologies 20
  - History 20
  - The Introduction of Metal 21
  - The Challenges of Tension 23
  - Space Frames and Shell Structures 26
  - Contemporary Connection Methods for Wooden Frames 28
- Design for Disassembly 31
- The Triakonta Connector System 35

Materials and Methods 38

- Overview 38
  - Modeling and Fabrication 39
  - Testing 46

Results: 49

- Summary of Results: 49
- Individual Trial Results: 53
  - Compression: Trial 1 53
  - Compression: Trial 2 54
  - Compression: Trial 3 56
  - Tension: Trial 1 58

Tension: Trial 2 59
Tension: Trial 3 61
Bending: Trial 1 63
Bending: Trial 2 64
Bending: Trial 3 65
Discussion: 67
Viability of the Triakonta System 67
Limitations of the Current Research 67
Design Implications and Areas for Future Research 68
Conclusions 71
References 73

List of Tables and Figures:

Table 1: Carbon emissions in representative building life cycle stages (p.13)
Table 2: Mechanical properties of Black Locust. (p.19)
Table 3: Reference Design Values for Visually Graded Timbers (p.67)
Figure 1: Three principal axes of wood with respect to grain direction and growth rings. (14)
Figure 2: Cellular matrix of wood, magnified 300X. (14)
Figure 3: Native range of Black Locust. (p.16)
Figure 4a-e: Common wood joint types. (p.21)
Figure 5: A simple triangulated truss (p.26)
Figure 6: Heydar Aliyev Cultural Centre (p.27)
Figure 7: Split ring connecter (p.29)
Figure 8: Toothed plate connector (p.29)
Figure 9: Multi-shear dowel joint in various configurations (p.29)
Figure 10: Hub type connector. (p.30)
Figure 11: Cowley connector member section. (p.30)
Figure 12: Cowley connectors in various configurations. (p.31)
Figure 13: Reduced energy and resource consumption in sample construction. (p. 34)
Figure 14: Rhombic Triacontahedron. (p.36)
Figure 15: Orthogonal reflection lines for the square, regular pentagon and regular hexagon. (p.36)
Figure 16: Full scale Triakonta system component assembly in section. (p.37)
Figure 17: Quarter scale Triakonta system component assembly in section. (p.41)
Figure 18: Detail of quarter scale node and strut. (p.41)
Figure 19: Quarter scale system assembled as chair. (p.42)
Figure 20: Milling jig for sleeve assembly. (p.43)
Figure 21: Completed strut assembly. (p.44)
Figure 22: Completed cone and node fixed to strut. (p.45)
Figure 23a: Complete testing apparatus (compression). (p.47)
Figure 23b: Complete testing apparatus (bending). (p.48)
Figure 24: Triakonta compression trial comparison (p.50)
Figure 25: Triakonta tension trial comparison (p.51)
Figure 26: Triakonta bending trial comparison (p.52)
Figure 27: Triakonta compression test 1 (p.53)
Figure 28: Longitudinal cracking at strut face (p.54)
Figure 29: Triakonta compression test 2 (p.55)
Figure 30: Yield failure at cone face (p.55)
Figure 31: Yield failure at node face (p.56)
Figure 32: Triakonta compression test 3 (p.57)
Figure 33: Off-center placement at compression plate (p.57)
Figure 34: Triakonta tension test 1 (p.58)
Figure 35: Shear failure of strut under tension (p.59)
Figure 36: Bending damage to steel cross pin (p.59)
Figure 37: Triakonta tension test 2 (p.60)
Figure 38: Splitting damage to strut under tension (p.60)
Figure 39: Bending damage to steel cross pin (p.61)
Figure 40: Triakonta tension test 3 (p.62)
Figure 41: Shear failure of strut under tension (p.62)
Figure 42: Bending damage to steel cross pin (p.62)
Figure 43: Triakonta bending test 1 (p.63)
Figure 44: Splitting failure of strut under bending (p.64)
Figure 45: Triakonta bending test 2 (p.65)
Figure 46: Splitting failure of strut under bending (p.65)
Figure 47: Triakonta bending test 3 (p.66)
Figure 48: Cracking failure of strut under bending (p.66)
Figure 49: Idealized buckling capacity of a fixed pin Triakonta long member (p.70)
Figure 50: Hexagonal section profile for the cone/node interface (p.71)

Introduction

Over the last couple decades, the topic and field of environmental sustainability has increasingly become a part of international discussion. While first relegated to national and international research organizations focused on determining the effects of human action on the earth's climate, the field and scope of environmental sustainability has emerged and grown in the public consciousness. The field of environmental sustainability now encompasses a broad range of ideals, practices, goals and protocols, all of which link to the increasingly shared realization that society has grown to the point where our actions can effect ecological systems on a planetary scale. It has also become apparent that without a clear understanding or consideration for our actions, irreversible damage to these systems is possible, which may comprise not only the ongoing viability of these systems, but our own viability as a civilization as well.

While numerous areas of research, touching all aspects of our environmental interactions are being investigated, a particular focus has been placed on the design and implementation of the built environment which supports our collective daily actions. The built environment and the artifacts which comprise it are both literally and figuratively the foundational elements of our interaction with natural systems. Decisions we make in the implementation and design of these buildings at every scale have a disproportionate impact on these ecological systems, and the expansion of both our understanding and capabilities in designing these artifacts is of critical value as progress is made in successfully integrating human and natural systems.

This research seeks to expand the knowledge of our capabilities in a key area of this design process, the development of environmentally benign architectural structures, built to support our human environments while satisfying both our ecological and human goals. Since the inception of the industrial age, incremental progress has been made in the development of these systems, particularly in the pursuit of optimizing cost. However, a new perspective which acknowledges and emphasizes the additional externalized environmental costs of these systems over the courses of their entire lifespans will be necessary as the industries of engineering, architecture and design adapt to meet the expectations of realities of a sustainable society. By exploring the use of alternative materials and designs that are predicated on doing less environmental harm, this research seeks to contribute to the development of that new perspective. Specifically, this research sets out to test the structural viability of a new wood-based building system designed by Professor Jack Elliott of Cornell University, known as the Triakonta Building System (TKBS) It allows for the replacement of carbon intensive building materials such as concrete, steel, aluminum and masonry with less carbon intensive wood alternatives and utilizes the principles of modularity and design for disassembly, as a means of reducing waste volume associated with deconstruction and increasing the end of use value and reusability of building products.

Background (Literature Review)

The Problem with Carbon

Gross concentrations of greenhouse gases (GHG) in the atmosphere are increasing at an ever accelerating rate. The total concentration of CO2 in the earth atmosphere was measured at 392ppm in 2011, almost 100ppm greater than pre-industrial levels, and the building industry is one of the primary emitters of greenhouse gases globally. According to the Intergovernmental Panel on Climate Change (IPCC) in their 2007 Climate Change Report, the building sector, which includes both the construction and operation of the built environment, including electricity, emitted over 8.6 billion tons of CO2, or approximately 25% of global CO2 emissions. It is in the building sector, however, that the greatest potential for reduction exists, with IPCC reporting a global potential for a 29% reduction in global baseline emissions in the commercial and residential sectors.

A second major problem facing the building and construction industry is the massive generation of waste attributed to the constant construction, renovation and demolition of the global building stock. In 2006 it was estimated that over 7.6 billion tons of industrial solid waste was being generated annually in the United States alone, 170 million tons of which can be attributed directly to construction and demolition (C&D) activities (U.S. Environmental Protection Agency, 2009).

By its very nature, the growth and production of wood works to sequester carbon from the atmosphere. In 1997 it was estimated that approximately 58.4 billion metric tons of CO2 were stored within the trees, biomass, soils, and other woody debris in the United States alone (Birdsey & Lewis, 2003, p5). In 2008, the amount of carbon sequestered annually by U.S forests was additionally estimated at approximately 150 million metric tons, roughly equivalent to 10% of domestic carbon emissions during the same time period (Negra, Sweedo, Cavender-Bares & O'Malley, 2008, p.1378-1379).

The use of wood as a structural building material can have profound impacts on the lifecycle energy and carbon balance of a building project. One study conducted by Buchanan and Levine (1999) used carbon equivalency coefficients, in conjunction with the embodied energy figures from a wide range of building materials to compare the carbon emissions and storage capabilities of wood with a number of different building materials in different building types in the New Zealand building industry. Their analysis showed that wood building required significantly less process energy than materials such as aluminum, steel and concrete, and found that the substitution of wood for these more intensive materials had the potential to reduce the emissions associated with the manufacture of building materials by up to 20%, equivalent to 1.5% of all the greenhouse gas emissions for the country.

In a second study conducted in 2002, Glover, White and Langrish produced a comprehensive review of embodied energy studies for wood, steel, and concrete, and compared their figures for embodied energy under a range of circumstances including individual base material production values as well as the embodied energy values for

entire structures made predominantly from a single material type. The researchers found that when comparing base material production values, the embodied energy figures varied with 8.9–59.0 MJ/kg for steel, 0.86–5.4 MJ/kg for concrete and 0.6–9.0 MJ/kg for wood, based on the study and production characteristics of the material analyzed. When looking at completed structures the differences between material types were more pronounced, with the researchers calculating an average of 232 GJ of embodied energy for houses made with wood construction, 396 GJ for concrete house construction, and 553 GJ for steel construction.

A third 2004 study conducted by Lippke, Wilson, Perez-Garcia, Bowyer & Meil as part of the Consortium for research on Renewable Industrial Materials (CORRIM) compared the total lifecycle energy and carbon costs for typical residential buildings in Minneapolis, Minnesota and Atlanta, Georgia using either wood, steel, or concrete structural construction methods. The research team found that when looking at the environmental performance across the life of the total building the wood frame construction methods had an embodied energy level 17% smaller than steel frame construction in Minneapolis (651 GJ vs. 764 GJ), and 16% smaller than the concrete building frame in Atlanta (398 GJ vs. 461 GJ). This performance difference increased substantially when focusing specifically on the substituted structural components with the steel frame utilizing 281% more energy than the comparable wooden structure and the concrete frame utilizing 250% more energy than the wooden frame. The more significant conclusions drawn by the study, however, were the comparison of equivalent carbon emissions between the different building cases. Summarized in table 1, when taking into account all equivalent carbon flows for the building materials, including

maintenance, heating and cooling, and wood's sequestration of carbon in its growth and production, the wood frame construction resulted in net negative carbon emissions in the Minneapolis home and substantially reduced emissions in the Atlanta home across the entire lifecycle of the structures.

Table 1 - Carbon emissions in representative building life-cycle stages.[a]

	Minneapolis house		Atlanta house	
	Wood frame	Steel frame	Wood frame	Concrete frame
	(metric tons)			
Emissions in mfg., construction & demo.	37.1	46.8	21.4	28.0
Emissions from biofuel	3.6	2.6	3.4	2.7
Emissions from maintenance	3.4	3.4	4.1	4.1
Emissions from heating & cooling	390	390	232	232
Subtotal of sources	434	443	261	267
Forest sequestration	(467)	(246)	(103)	(85)
Wood product storage	(22.4)	(11.8)	(17.1)	(14.1)
Subtotal of sinks and stores	(489)	(258)	(121)	(100)
Net emissions	**(55)**	**185**	**140**	**167**

[a] (Lipke et al, 2004, p.17)

These figures illustrate the dramatic savings in embodied energy possible through the utilization of low energy intensive materials such as wood as replacements for high energy metals and masonry. The opportunities for the reduction in wasted embodied energy will only be intensified as buildings begin to operate more efficiently with the advent of low energy lighting, heating, and ventilation systems. A Swedish study of ultra-high efficiency housing conducted by Thormark (2001) demonstrated that over a 50 year lifespan, over 45% of a building's total energy use was embodied energy, and that the reusability and recycling potential for this type of housing was between 35-40% of the building's embodied energy.

Wood as an Engineered Material

The most important characteristic that effects the utilization of wood in a structural setting is its classification as an orthotropic material. This means that unlike steel, concrete and other isotropic building materials the structural properties of wood are entirely independent across three mutually perpendicular axes; the longitudinal axis, or parallel to the wood grain, the radial axis, perpendicular to the wood grain in the radial direction, and the tangential axis, perpendicular to the grain but in tangent to the growth rings (Figure 1). These separate and multidimensional properties of wood vary significantly both intrinsically within a given wood species but also vary radically across various wood and species types, complicating structural analysis (Green, Winandy & Kretschmann, 1999, p. 1-3).

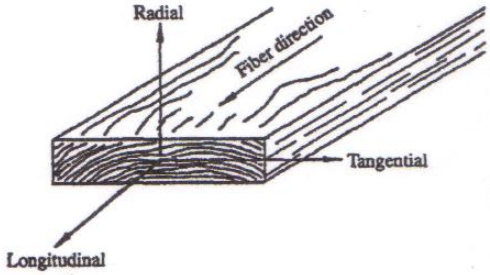

Figure 1: Three principal axes of wood with respect to grain direction and growth rings. (Green et al, 1999, p.3)

The primary reason for the complex structural mechanics of wood is the microscopic cellular matrix that forms the material. On a cellular level wood is composed of a highly complex and porous lattice of individual grain, cells and fibers which grow over time to form the plant structure. Chemically, wood is made primarily of cellulose, hemicellulose, and lignin, which form the plant cell walls. It is the size, shape, orientation and arrangement of

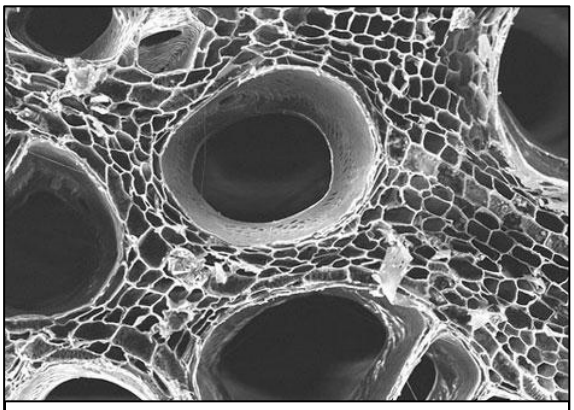

Figure 2: Cellular matrix of wood, magnified 300X. (McLaren, 2009)

these cells that give wood its exceptionally varied mechanical properties (Figure 2). While this living nature of wood complicates its structural analysis, it also grants some of wood's exceptional and unique properties, such as its outstanding workability, its very high strength to weight ratio, and its rapid renewability and ecologically benign disposal (Steurer, 2006, p.50).

Looking outside of the cellular structure of the material, the mechanical properties of wood are additionally affected by a myriad of natural characteristics and variables. The specific gravity of the wood sample, or its relative density in comparison to other wood species, natural knotting of the wood grains, which can inconsistently distribute mechanical load through the material's structure, the slope of the wood grain within a sample, the age of the wood sample at harvest, damage from birds, fungus, and insects, and most dramatically, the moisture content, can all substantially affect the mechanical characteristics of a specific sample. The implications of these variations mean that two identically size samples from the same wood species harvested from the same area can have measurably different performance as structural elements (Niklas, 1997, 265-267) (Green et al, 1999, p. 1-3).

Black Locust

Black Locust [Robinia Pseudoacacia] is a North American hardwood found widely in the temperate forests of the United States as well as in southern Canada, Northern Europe and select areas of Asia. The original range and habitat of the black locust within North America is the humid central eastern Appalachian range, spanning

from Pennsylvania to Alabama north to south, as far east as western Virginia mountain and as far west as the Ozark Plateau of southern Missouri, Oklahoma and northern Arkansas (Figure 3). Despite this limited native range, black locust has been successfully transplanted to a number of different climatic condition, and soil compositions throughout the world. Stands of black locust can now be found throughout the United States as the result of selected planting and cultivation, and the tree is even considered an invasive species in several states (Burns & Barbara, 1990).

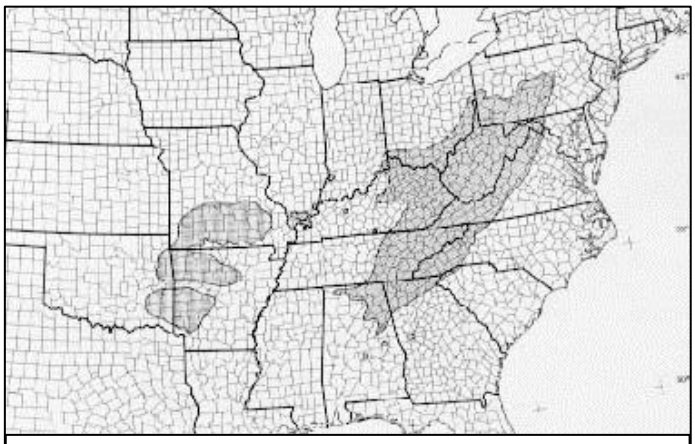

Figure 3: Native range of Black Locust. (Burns & Barbara, 1990)

A medium sized tree, typically standing between 40 and 60 feet and measuring 12-30 inches in diameter, the Black locust comes in dozens of different varieties and sub-species that are widely distributed. The most significant diversity of variants appears in Europe, with 49 different varieties being independently identified in Hungary alone. Modern genetic and protein analysis however has led to several of these varieties, such as the Ship-Mast Locust [Robinia Pseudoacacia var. Rectissima], to be identified for reclassification as ecological variants (Burns & Barbara, 1990).

While generally hearty, the two most significant threats to the Black Locust in the United States are the Locust Borer beetle [Megcallene Robiniae] and heart rot fungi [Phellinus Rimosus or Polyporus Robiniophilus] which can be introduced by the beetles into the core of the adult Black Locust tree (Burns & Barbara, 1990). These two

damaging agents are near ubiquitous in the United States, but are far less of a problem in Europe (Barrett, Mebrahtu &Hanover, 1990, p.278-283).

On the whole, black locust varieties share a number of traits which lend themselves to a variety of different uses in industry. The first such trait is Black Locust's rapid maturation and growth. Another is its capacity to fix nitrogen into surrounding soils, characteristic to other species in the Legume family. These two properties make the black locust a primary candidate for use in land reclamation, erosion control, honey production, as nurse crops, and in reforestation efforts (Burns & Barbara, 1990). More recently as energy production has come to the forefront of the national dialog in the United States, Black Locust has additionally been identified as a candidate for commercial biomass production, as it has the highest caloric density of all American hardwoods (Barrett, Mebrahtu &Hanover, 1990, p.278-283).

The second most notable trait of the Black Locust is its significant rot and insect resistance. Locust variants contain an unusually large concentration of flavonoids in the heartwood of the tree which is believed to impart this natural decay resistance. In testing, this natural resistance rivals many commercial wood preservatives (Barrett, Mebrahtu &Hanover, 1990, p.278-283). This distribution of flavonoids also contributes however, to a natural discrepancy between the durability characteristics of the heartwood versus newer growth, with the greatest decay and rot resistance being present in the heart and old growth areas of the tree. Overall Black locust is classified between a class 2 "durable" to class 1 "very durable" wood species according to the European En 350-2 (1994) wood durability standard, and is the only European

hardwood to meet this degree of durability, outclassing both the European oak [*Quercus robur* L.] and the European chestnut [*Castanea sativa* Mill.] (Pollet, Jourez & Hebert, 2008, p. 1366-1372). This makes the fast growing hardwood widely suitable for use in post making, mine timbers, ship timber, and railroad ties, with locust components lasting for decades in moist soils without significant degradation (Burns & Barbara, 1990) (Barrett, Mebrahtu & Hanover, 1990, p.278-283). It is important to note, however, that, despite its higher mean level of durability, individual wood samples can vary measurably as the result of the variation in the specific contaminant, species, genetic origin and site.

The last significant trait of locust varieties, which makes them desirable for structural applications, is their impressive mechanical strength and hardness. Black Locust lumber is one of the densest and hardest of any North American hardwood species. At 15% moisture content the wood is 49lbs per cubic foot, yet despite this high density is only minimally affected by shrinkage, unlike many North American hardwoods. It additionally is exceptionally strong in bending, with a modulus of elasticity over 2,000,000 psi (13,790 MPa) and a very high shock resistance rivaled only by true North American Hickories (USDA, 1971, p.3-6). A detailed table of the mechanical properties of black locust, as derived by the U.S. Department of Agriculture Forestry Service using small clear wood samples is shown in Table 2 (Green et al, 1999, p. 4-25).

Table 2: ----------*Static Bending*----------

Moisture Content	Specific Gravity	Modulus of Rupture (kPa)	Modulus of Elasticity (MPa)	Work to Maximum Load (KJ/m^3)
Green	.66	95,000	12,800	106
12%	.69	134,000	14,100	127
Moisture Content	Impact Bending (mm)	Compression - Parallel to Grain (kPa)	Compression - Perpendicular to Grain (kPa)	Shear - Parallel to Grain (kPa)
Green	1,120	46,900	8,000	12,100
12%	1,450	70,200	12,600	17,100
Moisture Content	Side Hardness (N)	Tension – Perpendicular to Grain (kPa)		
Green	7,000	5,300		
12%	7,600	4,400		

Overall, the suitability for Black Locust for structural applications is promising. Its natural strength and durability make it a prime choice for high strength structural applications looking to reduce reliance on more carbon-intensive structural materials such as steel. In addition, the use of locust reduces reliance on chemical wood treatments and preservatives. In the United States, however, the problems with the locust borer beetle and heart rot, as described above, have significantly impacted the utility of Black locust, both by significantly diminishing the prevalence of uniform straight timber growth and by potentially compromising the integrity of dimensionally large samples. Many areas of Europe, however, being unaffected by the borer and rot issues have taken full advantage of Black Locust as a valuable timber species (Barrett et al.,

1990, p.278-283). Research into the feasibility of genetically increasing the trees natural resistance to these pests through hybridization and selective breading has illuminated a promising potential for creating resistant strains of locust for North American exploitation, but no commercially scalable projects are currently underway.

The Evolution of Connection Technologies

One component of the structural system that has had a profound impact on the utilization of wood as a structural material is the evolution of connection technology that has facilitated new wooden forms and structural types. The design of wood structures is often limited not by the wood itself, but by the strength of the connections, and as a result progress in the utilization of structural woods has been dependent on the evolution and refinement of connection techniques and technologies (Steurer, 2006, p.52). While no one connection type exists that would satisfy the needs of all wooden structures, the evolution of structural connection types has largely defined the utilization of wood as a structural material.

History

One of the primary factors governing the development of wood connection techniques in early societies was the cost and scarcity of metals. The majority of early wooden connection systems utilized gravity, mechanical loads, or geometry, and simple mechanical fasteners to join wooden struts together. The simplest example of a wooden connection of this type is a simple Butt Joint. Created when one piece of wood is lain perpendicular to the end of another, this method of framing can be executed without any mechanical fasteners, utilizing gravity, or loading to maintain the connection, creating a doorway, wall opening or support columns. More sophisticated examples of this kind of

connection are the equally familiar examples of the housing joint, the bridle joint, the dovetail joint, and the mortise and tenon (Figure 4a-e).

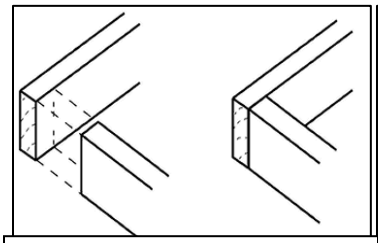

Figure 4a: Butt joint. (Timber, 2011)

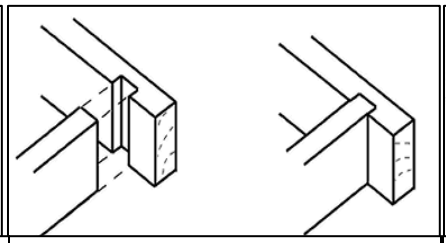

Figure 4b: Housing joint. (Timber, 2011)

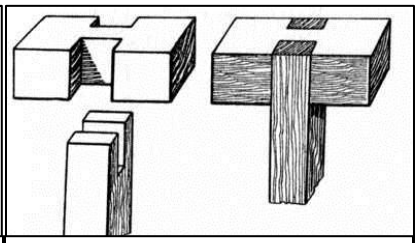

Figure 4c: Bridle joint. (Timber, 2011)

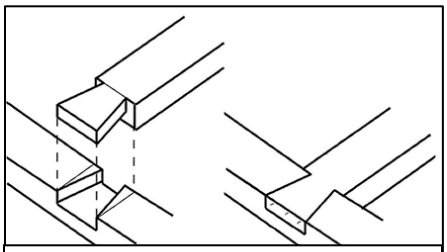

Figure 4d: Dovetail joint. (Timber, 2011)

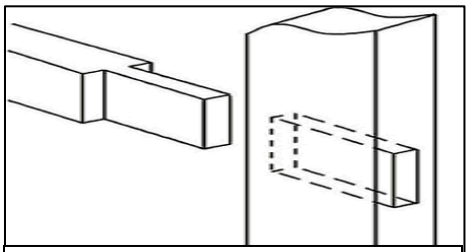

Figure 4e: Tenon joint. (Timber, 2011)

Hundreds of variations of these and other joint types, both with and without mechanical fasteners, such as dowels, pins, and shims permeate early architectural design, but what unifies this design typology is the lack of significant or structural metallic components. These joint types were widely used in developing societies and are still utilized widely today in timber framing, furniture making, and a multitude of other wooden structures, due to their economy of form and materials, their inherent simplicity, and their mechanical strength.

The Introduction of Metal

One of the fundamental developments in connection technologies for wooden structures was the introduction of metallic fasteners and connectors. One of the first and most prolific of these fasteners was the metallic nail. Originally composed of base metals such as Iron and copper, alloys such as bronze, and even gold in some more

decorative, non-structural instances (Nicholson & Shaw, 2000, p.149-172) the utilization of metallic nails dates back at least to Protodynastic Egypt at the beginning of the Bronze age around 3400 B.C . It was not until the early Romans, however, that iron smelting techniques were perfected, and that iron nails for minor structural applications became widely used around 1,000 B.C. (Bohl, 2001). There are even a number of references to nails in versions of the bible, “And David prepared iron in abundance for the nails for the doors of the gates, and for the joinings; and brass in abundance without weight” (Chronicles 22:3, Kings James Version).

It wasn’t until the 1400’s however, that the modern corollary to the nail, the metallic wood screw, began to be produced in Europe. Early wood screws were hand made from blanks by artisans working with files and chisels and were primarily used for furniture, and other high cost goods. It was not until the mass production of the screw during the industrial revolution that they became widely used as a suitable replacement for nails in minor framing and construction. The first patent related to machine manufactured wood screws dates back to 1760 England, which outlined a lathe based cutting method to produce wood screw for mass production (White & Christopher, 2005, p1-4).

Both the introduction of the nail and the screw had profound implications for the connection of wooden elements and the development of framing structures. However, before more modern developments in structural analysis and the quantification of building mechanics, the role of nails and early screws was regulated to more cosmetic and nonstructural applications.

The Challenges of Tension

One of the biggest stumbling blocks for early wooden structural systems and connections was tensile loads, or tension. Wooden connections and wood as a material itself were very strong under compression, but were far less predictable, with lower strength when in tension. Early fastener design such as wooden dowels and pegs were the earliest attempts to deal with tensile forces in wooden connection, but these systems were significantly weaker than the beams and struts used in the structures themselves, wasting resources, and leading to inefficient structural designs. Early engineers and architects attempted to avoid this problem by designing their wooden structures to be primarily compressive by nature, limiting their reliance on tensile connections (Streurer, 2006, p15-30). As the distances engineers attempted to span and the load requirements of the frames and trusses they were designing increased however, higher performing connection techniques and methods were required. Before these techniques could be implemented however, new models for structural analysis, testing and validation would be needed.

The first inklings of the transition to what today we consider modern structural analysis occurred in the mid-16th century. Scientists and engineers, frustrated by the constraints of the existing “rules of thumb” for design and construction, began to open their minds to experimentation and calculation as a means for interpreting the constraints of the physical materials. Many of the greatest minds of the era like Leonardo DaVinci began to push the boundaries of scientific understanding. During this time period the consolidation of general rules of thumb and principles of design to formal laws of mechanics had begun. Some of the first formal studies of structural

mechanics began with the study of materials by Galileo of Galilei (1564-1632). Building on the mathematical expressions for force developed by early astronomers such as Copernicus and Kepler, Galileo was the first to differentiate between the strength of a material, and the strength of a structure made from that material. He was also one of the first scientists to conjecture on the nature of material failures, wrestling with the difference between tension and bending forces and developed some of the first formal descriptions and rules for material properties and mechanics, devoting a large portion of his 1638 book, *Dialogues Concerning Two New Sciences,* to the subject. While many of Galileo's assumptions regarding structural mechanics appeared to be wrong, his work helped to stimulate further formal large scale studies done on materials characteristics, including notably the work of Robert Hooke (Addis, 2007, p.184-192).

Between 1662-1664 Hooke begun an extensive investigation of the properties of materials at the Royal Society in England. By this time he had already developed his now famous law of elasticity, and through the application of this law, and other principles, Hooke performed one of the most rigorous sets of evaluations of materials properties for his day, evaluating the strengths of not only common materials such as wood and metal, but glass, horn and hair as well (Addis, 2007, p.194). Hooke's work, along with other scientists working on the same issues such as French scientist Edme Mariotte (1620-84), demonstrated how to deal with the problem of bending and deformation in materials. This work ultimately lead to a revolution in the understanding of structural mechanics, by forcing the engineers who followed him to focus on two very distinct problems, the ultimate strength of materials, and the properties of stiffness and fracture.

It was during this time, in the early 1700's that the true value of this data and research was beginning to be widely understood. One the most important, if not widely known researchers into the strength of materials was a man named Petrus van Musschenbroek (1692-1761), who in the 1720's conducted some of the most comprehensive analysis of building materials ever published. Working during the same period as the more famous French Physicist René-Antoine Ferchault de Réaumur (1683-1757) who had conducted strength test on iron and steel, Musschenbroek published his book *Physicae Experimentales et Geometricae* which presented his testing results for more than 20 species of wood, iron, steel, and numerous other building materials, including the buckling loads of slender elements. In addition to this data, he experimentally determined the formulas for buckling loads more than 30 years before the more famous Leonard Euler (1707-1783) derived them mathematically (Addis, 2007, p.194-197).

It wasn't until the late 18th century and early 19th century however that what we consider to be the modern methods of structural analysis were finally completed. The scientists credited with the completion of these methods were Daniel Bernoulli (1700-1782) and Leonard Euler, who are credited with the development of classical beam theory and more complete mathematical methods for computing element behavior within a structure. Unfortunately for the field of carpentry, and structural mechanics, it would be many years before the research and rigor of the early scientists working in materials and structural mechanics would be applied to the general construction industry. One of the primary reasons for the slow adoption of these methods and techniques was the complexity of their formulation, calculation, and utilization. Most

builders during the time periods of these scientists found the majority of their work incomprehensible (Streurer, 2006, p32, 38). It was not until the work of Claude-Louis Navier (1785-1836), and his creation of a mathematically usable form of the general theory of elasticity, his discovery of the zero line of mechanical stress, and his establishment of the elastic modulus as a separate material property in 1826, that an accurate set of analytical tools could begin to be broadly applied to the building and construction field (Navier Biography, *2000*).

Space Frames and Shell Structures

The development of accurate methods of structural analysis by Navier and his predecessors, and advances in joining and connection techniques for structural elements helped to facilitate the creation and utilization of more efficient structural forms. Likely the most significant development in structural mechanics formalized by these tools was the triangulated truss. In the strictest sense the truss is a two dimensional assemblage of linear elements, connected by pins, in a triangulated pattern (Schodeck, 2006, p.10). The natural stability of the triangle, in conjunction with the pin connectors results in the complete distribution of applied forces as pure axial loads, tension and compression in which most conventional materials are strongest (Figure 5).

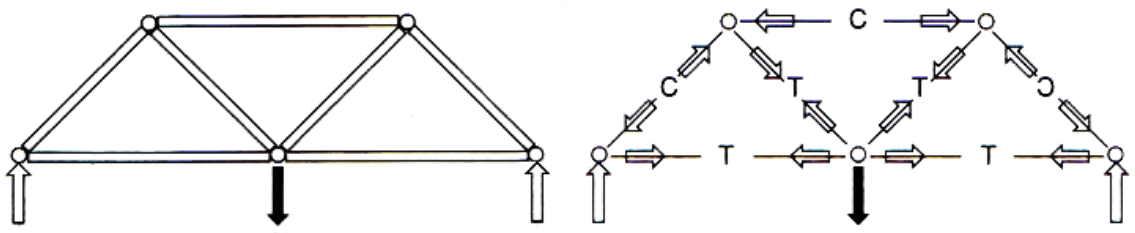

Figure 5: A simple triangulated truss. (Schodek, 2006, p.154)

This configuration results in an extremely efficient utilization of materials and was heavily utilized by 19th century architects and engineers in the development of bridges and other long structural spans.

Replacing the idealized pin type connections with a rigid connection results in a triangulated frame which, while sacrificing a purely axial distribution of load and introducing bending and shear forces into the structure, allows for non-triangulated elements, such as rhombi and hexagons, and facilitates the extension of the truss into three dimensional frame, or space frame. Space frames utilize three-dimensional polyhedra to create geometrically complex yet structurally efficient load bearing structures. Since their inception, space frames have come to dominate the field of wide space structural engineering as well as other sectors where a premium is places on a high strength/weight ratio (Figure 6).

Figure 6: Heydar Aliyev Cultural Centre (Dispenza, 2011)

The majority of modern space frame systems today are made using metal components made primarily from steel and aluminum. The strength and workability of steel and aluminum combined with the efficiency of the space frame structure allowed for very large and efficient structural forms to be realized. In recent years, however, as a greater emphasis has been placed on embodied energy and environmental performance, engineers and architects have begun to evaluate wood as an alternative material for these framing systems.

As mentioned previously one of the primary problems with incorporating wood into these systems has been interfacing wood and metallic components. Early on in the development of wooden space frame systems, engineers learned quickly that due to the distribution and application of forces within the typical space frame system and the orthotropic nature of wood as a material, wood performs well under the primarily axial forces, as experienced within the strut components of the frame, but the complex forces experienced in the node components which tied the different struts together still required the strength and uniform performance of metal in most cases. Unlike their entirely metallic predecessors, which often utilized welded connections throughout the space frame, the introduction of wooden components into space frame systems required a newer and more versatile class of connection systems to facilitate their use.

Contemporary Connection Methods for Wooden Frames

As development in modern structural systems progressed, new connector types were developed to accommodate these structures. Some of the earlier developments in connection technologies were the split ring connector and toothed plate connector. These connector systems, part of the larger class of shear connectors, relied on pressing the ring or plate between bolted wooden struts, relying on the resulting resistance to shear to provide structural stability (Figures 7 & 8).

Figure 7: Split ring connecter
(Harris, 2011)

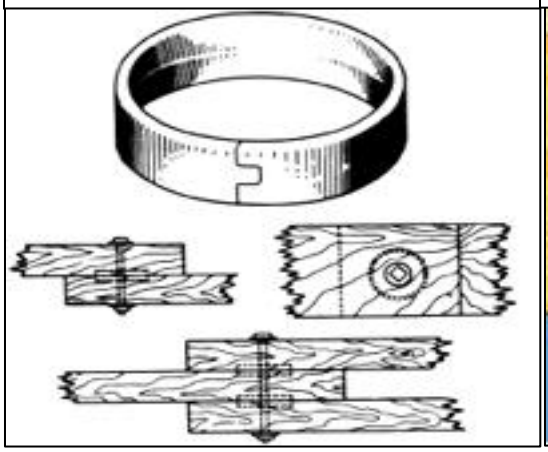

Figure 8: Toothed plate connecter
(Connectors for Construction, 2011)

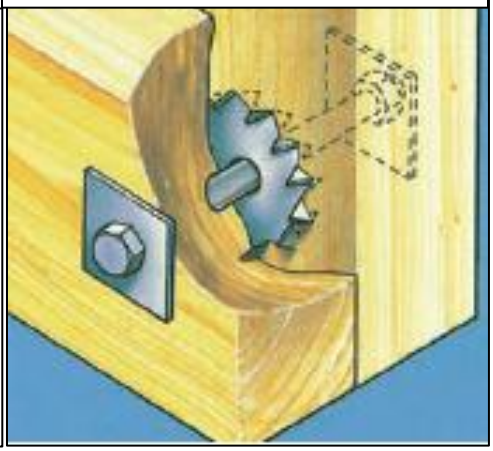

Later on in the 1980's and 1990's research into timber engineering and truss design at the Swiss Federal Institute of Technology Zurich (ETH Zürich), lead to the development of the multiple shear dowel joint. The product of years of theoretical research on the mechanics of loading and stress in wooden trusses, this joint utilizes pinned shear plates on the exterior and interior of the wooden strut to create secure interfaces between struts. This design creates a strong and reliable connection which has been implemented in numerous configurations in truss design (Figure 9) (Streurer, 2006, p54).

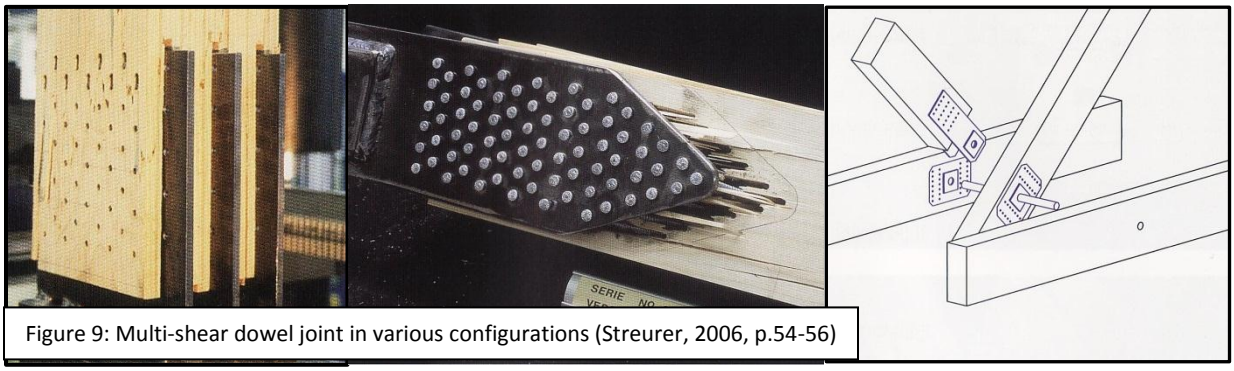

Figure 9: Multi-shear dowel joint in various configurations (Streurer, 2006, p.54-56)

These connection types have been optimized primarily for use in two dimensional trusses and frames, but as engineers have begun to incorporate wood into complex space frame and shell structures, many new developments in connections and interfaces, some drawing on these more conventional techniques, have been introduced. The first of these techniques is the hub connection. This connection type utilizes a series of brackets or multi-shear dowel joints rotated around a central hub. This allows the creation of complex dome systems and shell structures, with the hub providing strength and support for the wooden struts (Figure 10).

Figure 10: Hub type connector. (Geodesic Dome, 2011)

Some of the most recent examples of complex wooden space frames however, have utilized a completely new connection mechanism for their construction. Developed by Cowley Timberworks in the United Kingdom, the Cowley Connector utilizes a captive bolt, held inside an epoxy bonded tube within the body of the wooden strut. The bolt is accessed and tightened through a small channel cut in to the strut body, which facilitates quick assembly and disassembly (Figure 11). The Cowley Connector can be embedded into rectangular or cylindrical struts, and affixed to any node geometry with a corresponding threaded connection (Figure 12). The benefits of the Cowley system is that is facilitates rapid on site assembly and disassembly of the factory produced struts and nodes. While

Figure 11: Cowley connector member section. (Cowley, 2011)

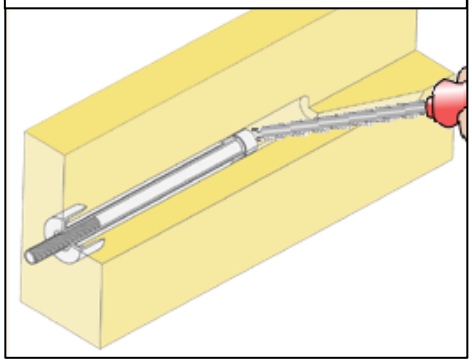

the system has not yet been implemented in a full scale structural space frame, it has been utilized in numerous grid and shell structures to great effect, and is readily adaptable.

Figure 12: Cowley connectors in various configurations. (Cowley, 2011)

Design for Disassembly

In addition to replacing traditional building materials with less energy intensive alternatives, the effort to reduce the embodied energy of the built environment has begun its focus on a second promising strategy, the principle of Design for Disassembly (DfD). More commonly found in the industrial design sector, this principle calls for the optimization of a design of building systems to facilitate their disassembly and reuse, either after the products useful life ends, as a means of facilitating the recycling process, or as a means of continued reuse for building components, increasing product flexibility, scalability, or deployability. While a somewhat foreign concept to the cradle to grave building model ubiquitous to the modern global industrialized building sector, this principle has been utilized throughout history to address production and resource constraints similar in character to macro-scale materials and energy pressures society faces today.

In the area of building structures, the nomadic tent is the archetypal example of this principle; a light, portable and collapsible frame that provides a strong and rigid support structure for a flexible and protective membrane. Other examples include the historical salvage and reuse of wooden structural beams in areas where either wood was scarce, such as in many areas of northern Africa and the Middle East, or where production costs were high such as Europe in the Middle Ages. Modern building materials share a connection with these older forms in that the structural materials and components themselves far outlive the isolated building cases we use them in and with simple changes in design, substantial savings in materials and production costs can be realized.

Traditionally, building energy research has focused primarily on the reduction of operational energy consumption to reduce total energy use. This is largely due to the perception that the overwhelming majority of a building's total energy is consumed during the operational stage of its life. Recent research, however, has shown that the embodied energy of a building plays a much larger part in a building’s total energy consumption than initially thought. The embodied energy of a building can be defined as the sum total of the energy required to produce the materials used in a building construction, the energy for the construction process itself, the total energy contained in the materials used in or by the renovation process for that building, and the energy required to demolish and process the building at the end of its useful life. In short, embodied energy roughly corresponds to all non-operational energy associated with the building.

In contradiction to the general assumption of operation energy versus embodied energy, a 1999 paper by Philip Crowther presented at the 16th International Conference on Passive and Low Energy Architecture in Melbourne Australia found that the total embodied energy in a building can easily approach 30% to 40% of its total lifecycle energy use over 40 years, and that 20-50%, and 50-70% of that energy is held within the building structure and envelope respectively. This same study reported that in Australia's building sector as little as 11% of demolished commercial offices building materials are reused and 58% are reprocessed, leaving 31% of total building materials to be dumped in landfills. This translated into roughly 45% of the buildings total embodied energy going to waste (Crowther, 1999).

A second 2001 Japanese study, conducted by Weijun Gao, Takahiro Ariyama, Toshio Oijum and Alan Meier reviewed the potential for energy and materials savings through reclamation and reuse methods in residential construction. The research focused on three different construction styles, conventional wooden construction, wood frame construction, and light steel construction. These construction styles were evaluated against three different recycling and reuse methods, using entirely new building components, using recycled building components, and using recycled components with a salvaged and reused building structure. The researchers found that by utilizing recycled and reused components, over 10% of the total energy consumption could be saved overall, and a greater than 50% reduction in disposed materials could achieved when compared to conventional practices. The greatest energy savings were achieved in light steel residential construction cases with a reused frame, due to the large embodied energy of steel and other metallic components. The greatest material

savings were seen in conventional wooden construction and were also achieved through reuse of salvaged building structure (Figure 13). The research shows the distinct advantages in energy and materials through the utilization of reusable building structural components.

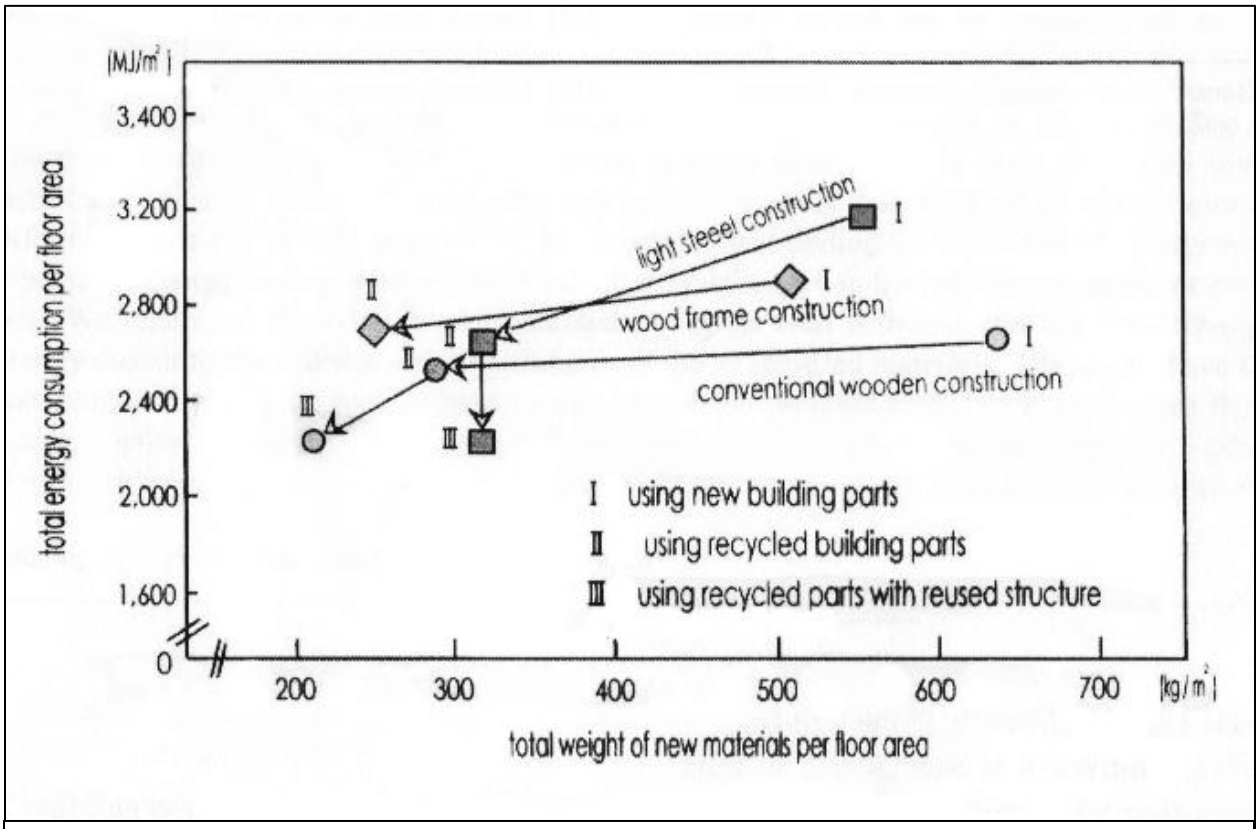

Figure 13: Reduced energy and resource consumption in sample construction. (Gao et al, 2011, p.561)

A third 2000 overview report, "Overview of Deconstruction in Selected Countries" published by the International Council for Research and Innovation in Building and Construction (CIB) and the Center for Construction and Environment at the University of Florida, numerous researchers from around the world reported on the state of their respective countries construction waste industry and the proliferation of demolition salvage and re-utilization programs. The general consensus of the forum was the need for a paradigm shift in construction waste disposal. While some countries such as

Australia and Denmark have achieved recycling and reclamation rates for construction materials >90% in some areas, most countries have not implemented comprehensive or effective building waste management programs (CIB 252, 18, 145). The financial drives for such programs are increasing around the world. The EPA for example estimates that tipping fees in the United States are increasing as much as 7% annually on average, with the cost of landfilling exceeding $110/ton in space constrained metropolitan areas such as San Francisco (CIB 252 191-193), an upward trend which is reflected throughout European metropolitan areas as well.

As environmental awareness and the need for building materials reclamation and landfill diversion increases, developments in building design and construction methods which focus on facilitating disassembly, durability and reuse will dramatically increase the effectiveness of materials reclamation, recycling, and reuse programs.

The Triakonta Connector System

The connection system developed for this project was devised to try and integrate the principles of low carbon materials, and structural flexibility and reusability into a full scale building framing system. The system uses a strut / node relationship, with unique node geometry, and three standard strut lengths to create a morphologically versatile framing system that can be deployed in a number of different settings, from the creation of shell structures, to planar space frames, which can be used in flooring or roofing applications.

The system as a whole is inspired by the popular molecule and space frame construction set made by ZomeTool, which exhibits an extraordinary geometric

versatility in geometric construction using single “Zome” node geometry based on the 62-faced small rhombicosidodecahedron and 13 unique, yet related struts lengths. For the Triakonta system a simpler system was developed working with a 30-faced rhombic triacontahedron, a complex polyhedron that has thirty uniform rhombi as its faces (Figure 14). This geometry is the same found in “D30”, thirty sided dice, used in many popular role-playing games. In addition to reducing the complexity of the node, the geometry of the struts resulting from inter-connecting the triacontahedrons is also less complex. A complete structural system can be produced with a total of three strut lengths, simplifying the total system to four basic components while still allowing for highly versatile construction geometries. Much of this versatility comes from the node’s ability to demonstrate two-fold, three-fold, and pentagonal or five-fold symmetry (see Fig. 15). Often overlooked due to its virtual absence from standard studies of crystalline structures, such as most atomic solids and metals on which traditional studies of symmetry were based, pentagonal symmetry is widely found in biological systems, such as plants and molecules, music, and art (Hargittai, 1992, p.1-30).

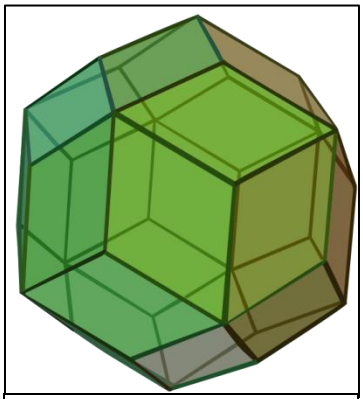

Figure 14: Rhombic Triacontahedron

Figure 15: Orthogonal reflection lines for the square (two-fold), regular pentagon (five-fold) and regular hexagon (three-fold). (Hargittai, 1992, p.6)

In addition, the golden ratio is embedded throughout the Triakonta system. The golden ratio exists when the ratio of the sum of two quantities to the larger quantity is the same as the ratio of the larger quantity to the smaller quantity, and is expressed as an irrational mathematical constant with the lowercase Greek letter phi **φ.** This ratio is found in numerous instances in nature, art, music, and architecture. For example, each rhombic face of the rhombic Triacontahedron is a golden rhombus, meaning the ratio of its longitudinal axis to lateral axis is the golden ratio, or approximately 1.618:1. This ratio is also demonstrated when comparing the three strut lengths that result from connecting the triacontahedral nodes, As a result, surprisingly complex and varied geometric morphologies can be created through the utilization of only four base components.

The connector mechanism itself is an internally constrained bolt situated inside a metal sleeve which is fastened to the cylindrical strut with two dowel pins. The bolt itself utilizes a small cross pin which allows the bolt to be turned by spinning the cone. When tightened the bolt creates a threaded connection to the node face. The geometry of the tapered strut end and conical tip allow complete positional freedom for struts around the node faces, including faces immediately adjacent to one another (Figure 16).

Figure 16: Full scale Triakonta system component assembly in section.

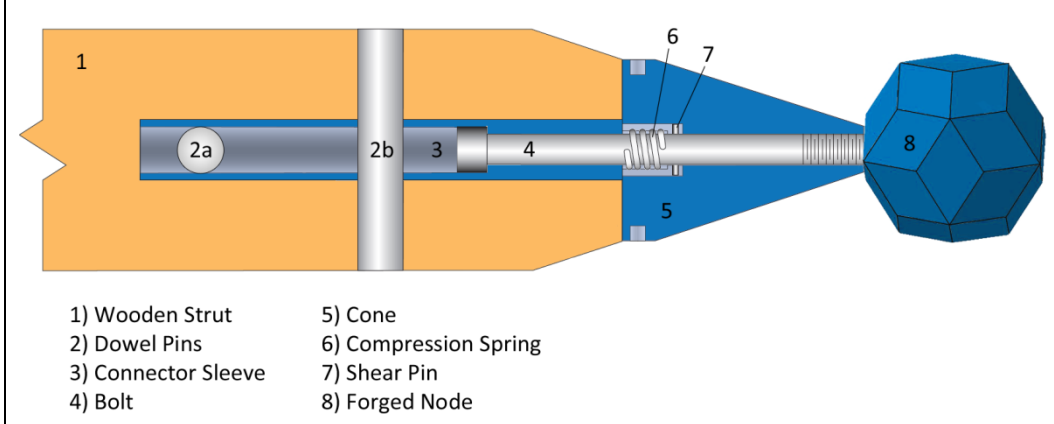

This particular design is unique from similar connector systems such as the Cowley Connector in two ways. Firstly, it is a completely dry assembly and disassembly system which requires no wet processes, such as adhesives or epoxies, to complete the connection. The sleeve is bolted to the wooden strut using two cross dowel pins. This allows for complete, non-destructive disassembly at the end-of-life. Secondly, the connector system is internally isolated as well, meaning that once the connection assembly has been fixed to the ends of the wooden struts, no dedicated access to the internal bolting mechanism is required to facilitate the tightening and loosening of the bolt. Instead, the mechanism is operated with a single pin wrench that engages in the perimeter holes of the cone.

Materials and Methods

Overview

The research unfolded in two main phases; the modeling and fabrication of Triakonta framing system with an emphasis on material utility and fabrication methods, and the full scale trial testing of prototype assemblies in the Bovay Civil Infrastructure Laboratory Complex.

The modeling and fabrication phase of the research took place in two stages. The first was the fabrication and testing of a quarter scale version of the system. This allowed us to determine the viability of the geometry, the workability of Black Locust as a structural material, and to test the design details before fabrication of full scale structural prototypes. The second stage was the fabrication of full scale prototype elements in the Emerson Product Realization Lab. While the metal components of the

prototype connector assemblies were fabricated in this lab and associated machine shop, several the wooden struts used in the prototype trials were contracted to third party workshops due to limitations in materials, tools, and time.

The prototype testing phase was additionally broken into two sub-stages. The first stage of the testing phase was the creation of the mechanical testing protocol, which was developed with the help of Tim Bond, Manager of Technical Services at the Civil Infrastructure Laboratory Complex. As part of the development of this testing protocol, Tim assisted in the specification of appropriate loading, fixing, and measurement apparatus for the proper testing of the axial tensile and compressive strengths, and bending strength of the connection system. In the second stage all struts were tested to failure to determine the potential viability of the system in real world structural applications.

Modeling and Fabrication

Quarter Scale Modeling

Before the final development of the full scale Triakonta system design, scale models of the system were created to test the base conceptual viability of the materials and system geometry. The scale models, while generally representative of the larger Triakonta system, incorporated several material and design differences which helped to facilitate large volume fabrication (Figure 17).

Unlike their full scale counterparts, the nodes of the scale system were cast from aluminum. Limitations in funding and tooling capabilities meant that the fabrication of the nodes in steel would have been cost prohibitive, so a single aluminum prototype

was contracted to a third party fabricator and used as the master pattern for investment casting of the scaled nodes in aluminum. The scale nodes were then hand ground to remove stubbing and provide uniform surfaces. To complete the node production, all faces of each node were drilled and tapped.

The struts for the scale system were created from rough cut black locust dimensional lumber. The lumber was sawn into 2 x2 inch (50.8 x 50.8mm) square sections, and then sawn again at 45° on each edge to create on octagonal section approximating a cylindrical profile. The struts were then cut to their corresponding strut lengths. The primary strut length for the scale system was 17.71 inches (450 mm) when measured from center to center of its corresponding nodes. The other lengths were created to be golden sections, one larger, one smaller, of this primary length. The ends of the struts were then chamfered with a tenoning tool, and completed by center drilling and boring each end to accommodate the connection sub-assembly (Elliott, 2010, p.4). The connector assembly was made from an aluminum bolt constraining sleeve pinned to the wooden strut using a single 2” stainless steel dowel pin. A stainless steel washer and nut were added to the protruding bolt face and the nut was secured to the bolt using a chemical adhesive. Lastly, a hexagonally broached stainless steel coupling nut was added to act as the interface between the strut and node, approximating the cone component from the full scale model.

Figure 17: Quarter scale Triakonta system component assembly in section.

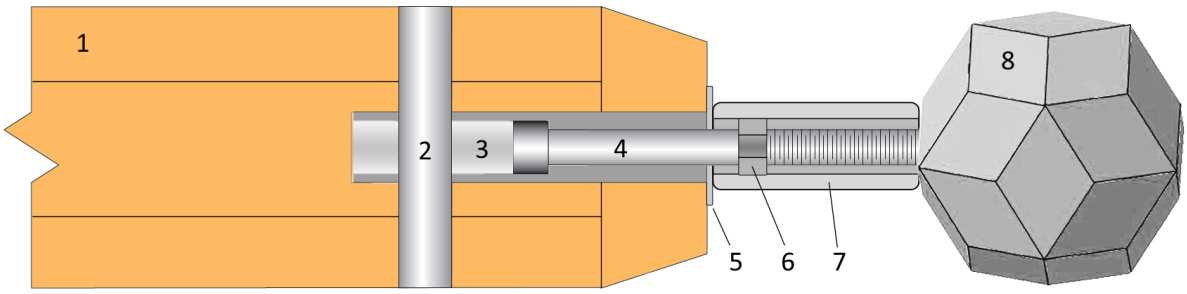

1) Wooden Strut
2) Dowel Pin
3) Bolt Sleeve
4) Bolt
5) Washer
6) Hex Nut
7) Broached Coupling Nut
8) Cast Aluminum Node

After fabricating of a large number of the scales strut assemblies of all three strut sizes as well as the nodes, a large number of configurations and geometries could be tested to verify the conceptual and geometric viability of the system (Figures 18 & 19). The only tool required for this assembly was a box end wrench to fit to the coupling nut.

Figure 18: Detail of quarter scale node and strut.

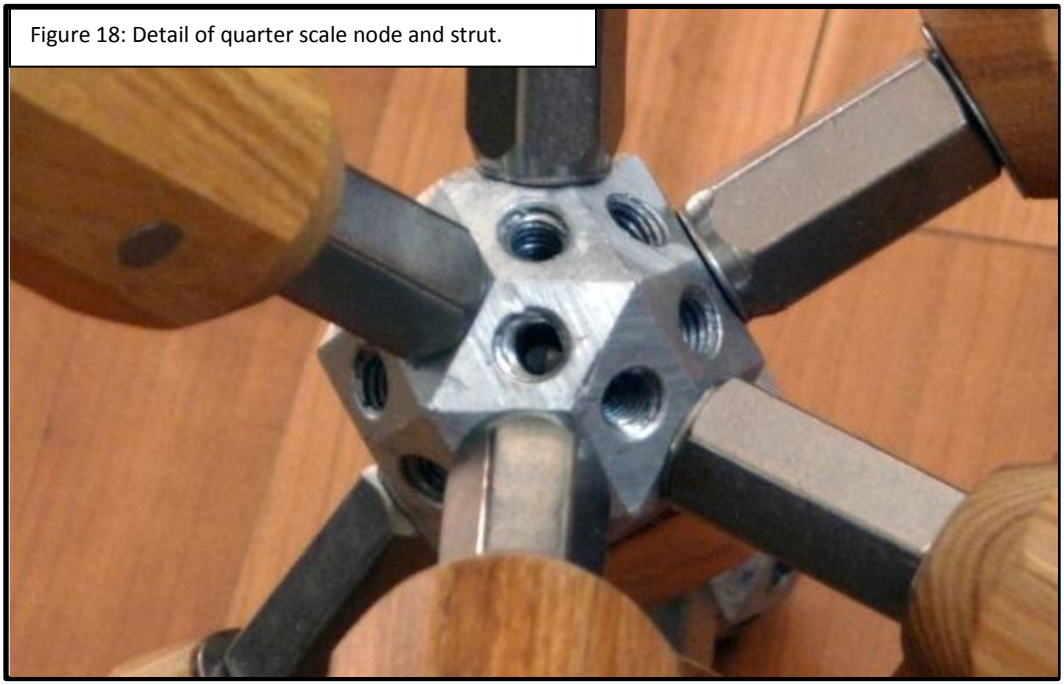

Figure 19: Quarter scale system assembled as chair.

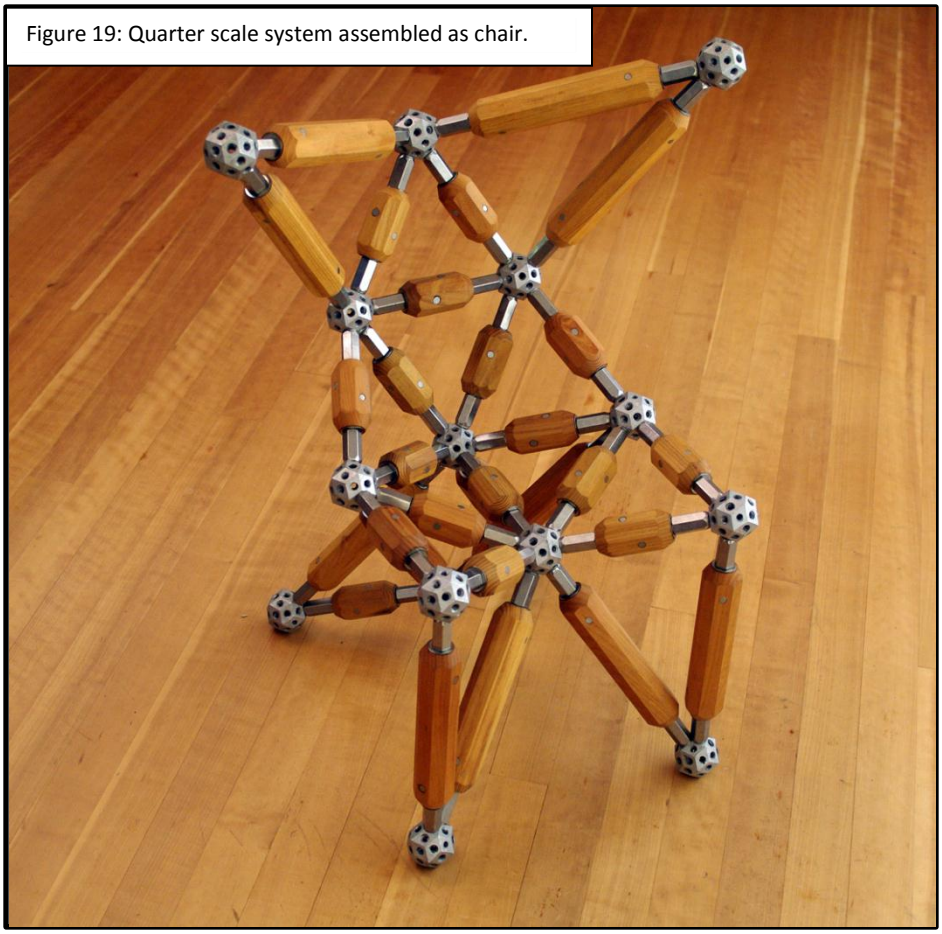

Once the proof-of-concept models had been created and tested the second stage of full scale prototype fabrication was started.

Full Scale Fabrication:

The full scale prototypes, which were to be used for mechanical testing, differed from the quarter scale models in several ways. Similar to the proof-of-concept models the full scale utilized black locust lumber as the primary material for the wooden struts, but for the full scale prototypes all of the metallic components for the system were fabricated from steel.

Due to resource constraints, only nine full scale struts were fabricated for testing. For the same reasons only two steel cones, two partial nodes and six sleeves were

fabricated for structural testing. Our working assumption during fabrication was that the wooden struts would fail long before the steel connection and nodes, allowing for reuse of the steel components throughout the testing process.

The struts were made from un-seasoned Block Locust logs, sourced from a local lumber supplier. Each log was specifically chosen to allow for full 8” diameter completed samples with the minimum amount of waste material during fabrication. Each log was then lathe turned to an 8” (203.2 mm) uniform diameter. Once turned, each log was cut and faced to a 36” (914.4 mm) total length, and chamfered at 18° to 6” (152.4 mm) on the strut face. Each strut was then bored with 2” (50.8 mm) drill 14” (355.8 mm) into each face of the struts. The final step in the creation of each strut was the milling of 1” (25.4 mm) pin holes at 5” (127.0 mm) and 12” (304.8 mm) from each strut face. The two holes were drilled perpendicularly from one another through the strut and required the creation of a custom jig for the mill, to ensure uniform production (Figure 20).

Figure 20: Milling jig for sleeve assembly.

The steel sleeves for the full scale samples were created from 14” (355.8 mm) length of 2” (50.8 mm) OD, 1” (25.4 mm) ID steel heavy wall pipe. Each sleeve was lathe bored to 1.5” (38.1 mm) ID, to a depth of 11.5” (292.1 mm), with the final 2.5” (63.5 mm) of the sleeve length lathe reamed to 1” (25.4 mm) to ensure free rotation of the bolt. As with the wooden struts, two 1” (25.4 mm) dowel holes were milled perpendicular to one another 5” (127.0 mm) and 12” (304.8 mm) from 1” (25.4 mm) ID sleeve face. Before each sleeve mechanism could be completed, a 12” (304.8 mm) Grade 8 socket head bolt was inserted into each sleeve, 1.25” (31.75 mm) long 1” (25.4 mm) ID steel compression spring was slid onto the bolt and a 1.5” (38.1 mm) steel cross pin was drilled and pressed into the bolt body 4.25” (133.35 mm) from the base of the bolt cap. Once completed, each sleeve mechanism was inserted into a strut such that their respective pin holes were aligned, and two 8” (203.3 mm) long 1” (25.4 mm) diameter Grade 8 steel dowel pins were mechanically pressed through the strut and sleeve body to secure each sleeve mechanism into the strut (Figure 21).

Figure 21: Completed strut assembly.

The two cones and two partial nodes were lathed and milled from 6”x8” and 6”x6” cylindrical blocks of low carbon steel respectively. Each cone was center drilled and reamed to 1” (25.4 mm) and had a taper turned at 18° to 1.5” (38.1 mm) OD at the smaller face. The cone was then counter bored to 1.5” (38.1 mm) diameter and 1’ (25.4 mm) depth from the larger cone face. Channel slots were then milled 2” (50.8 mm) into the cone to accommodate the bolt cross pins and allow tightening of the bolt mechanism. Four additional .5” (12.7 mm) holes were added to the cone collar. The node blocks were then faceted to replicate a single triacontahedral face and were drilled and tapped to 1” (25.4 mm), to a depth of 1.75” (44.45 mm). By sliding the cone over the strut assembly at each of its two faces, the prototypes could be secured to the partial nodes using a single fixed pin spanner wrench (Figure 22).

Figure 22: Completed cone and node fixed to strut.

Testing

Once fabrication was completed, the testing phase of the full scale prototypes could be completed. The testing was broken into three load conditions: compression, tension, and bending, in that order. Three samples would be tested under each loading condition.

Testing Apparatus & Protocol

The primary testing apparatus for all loading conditions was a SATEC Baldwin BTE400 universal testing machine. The Baldwin can provide a maximum of 400,000lbs (400 Kips, 1779 KN) in tension or compression. Load is applied through an oil based hydraulic piston, the head of which is the loading table or upper cross head. This loading is applied against a center cross head. The system is calibrated to measure loading in four distinct ranges; 400Kips, 80Kips, 16Kips, and 4Kips. Each range is independently calibrated to within .25% of its respective maximum. Applied force was measured with a National Instruments PXI-SCXI system and electronic pressure sensor integrated with the Baldwin. Displacement was measured with a 40” spring potentiometer calibrated using a rotary stepper motor/lead screw calibration system. The total calibrated precision of the testing apparatus was better than 200 lbs for tension and compression, and better than 40 lbs for bending. The measurement precision of the string potentiometer is .004 inches. The load frame itself is controlled manually with the attendant able to view both the current applied load and displacement relative to the loading platen. All testing software was written by Mr. Bond using the National Instruments Development Package LabView.

The tension and compression tests were performed at the 400 Kip range. The compression test placed the sample in the loading frame between the loading table and a plate positioned in the center of middle cross head, with pressure being applied by the loading table (Figure 23a). Rope was used to stabilize each prototype laterally to increase lab safety but was loosely tied to prevent interference with the load frame. The tension tests were performed by securing the nodes to grippers positioned in the center of the middle and upper cross heads, with pressure being applied through the upper crosshead of the loading frame. Rope was again used for lateral stabilization and safety.

Figure 23a: Complete testing apparatus (compression).

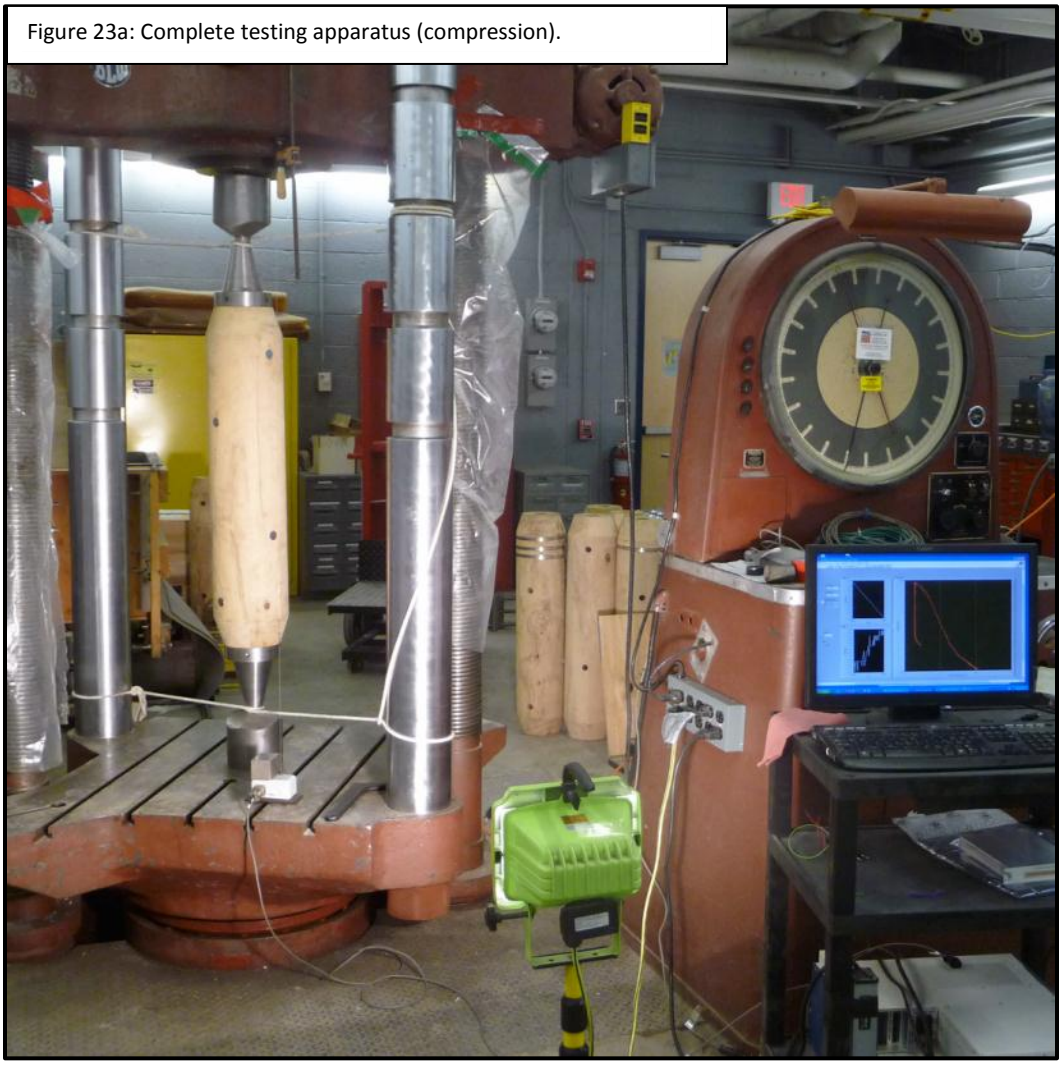

The bending tests were conducted at the 80 Kip range. A large steel girder was placed on the loading table to accommodate the length of the samples. Each sample was placed atop the girder in a set of steel V-blocks to prevent lateral rotation. The V-blocks were then placed on a pair of steel rollers to allow free rotation of the nodes. Due to fears of crushing damage on the strut face, a fitted steel distribution plate was fabricated to more evenly distribute the applied load through the center of the strut. A third roller was then place between the central plate of the middle crosshead of the load frame and the distribution plate (Figure 23b). The rollers were included so as to approximately replicate loading conditions for a simply supported beam.

Figure 23b: Complete testing apparatus (bending).

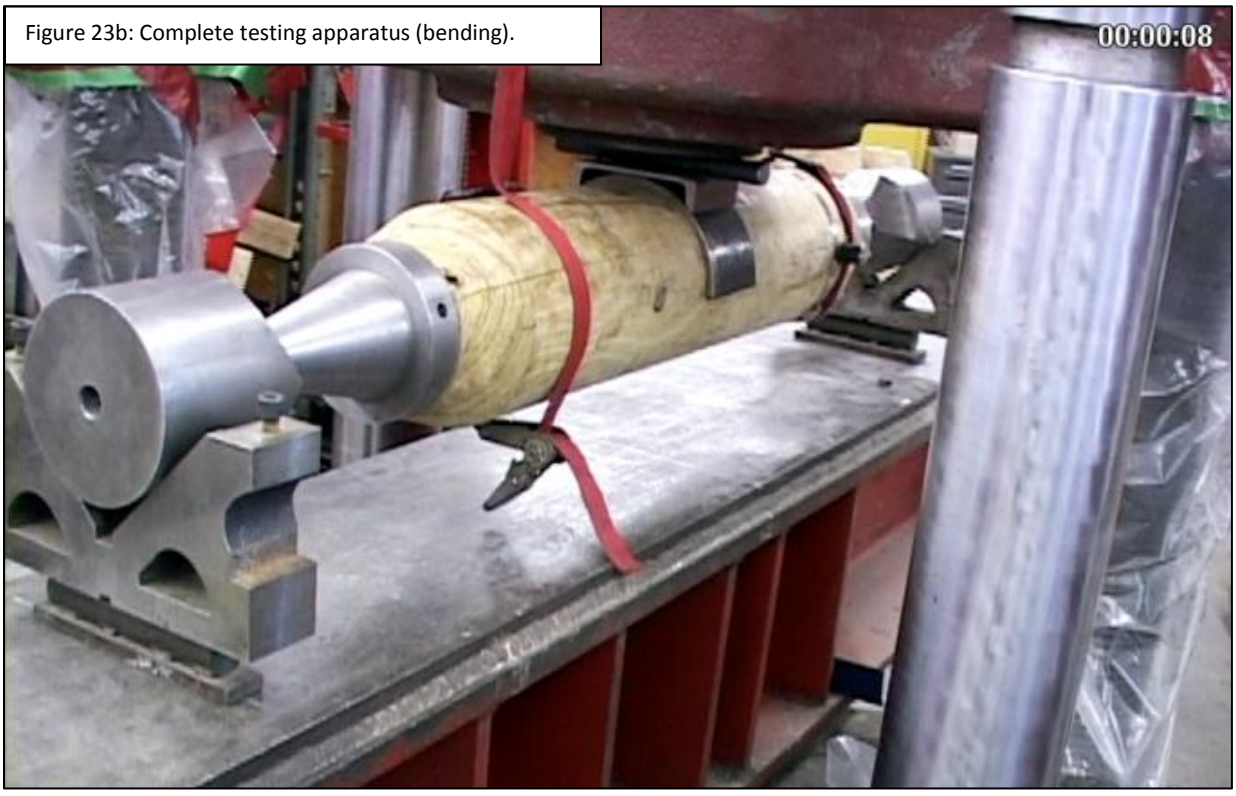

Results:

Summary of Results:

The mechanical properties of the connector assembly varied across the different trials for the different load types, but there were observable consistencies in performance and behavior. When looking at the compressive loading condition, the total loading capabilities varied significantly, from a low of ~60,000 lbs in the third trial to a high of over 140,000 lbs in the second (Figure 24). The reduced loading capacity of the first trial was manifestly due to the decision to discontinue loading of sample beyond 112,000 lbs. This can be contrasted to the second trial which was intentionally loaded until total structural failure. Despite minimal cracking observed in the wooden struts of the samples, contrary to our preliminary assumption regarding the system, the primary failure mechanism of the assembly, when taken to failure under compressive loading, was the yield failure of the steel cone, node, and bolt at the cone/node interface. Further investigation showed that this was not the result of a design deficiency. It resulted from the experimental setup where samples had been positioned off center within the testing apparatus. This unanticipated damage to the sole cone and node required repair in order to facilitate their reuse in the remaining trials.

In addition to the observed variability in total maximum loading capability, there were observable differences in the total deformation of the samples under loading, with the third trial displaying more than twice the total displacement per pound of loading than either of the first and second trials. Total displacement of the samples and the permanent deformation of the wooden struts however were significantly lower than in either the tensile or bending loading conditions.

Figure 24:

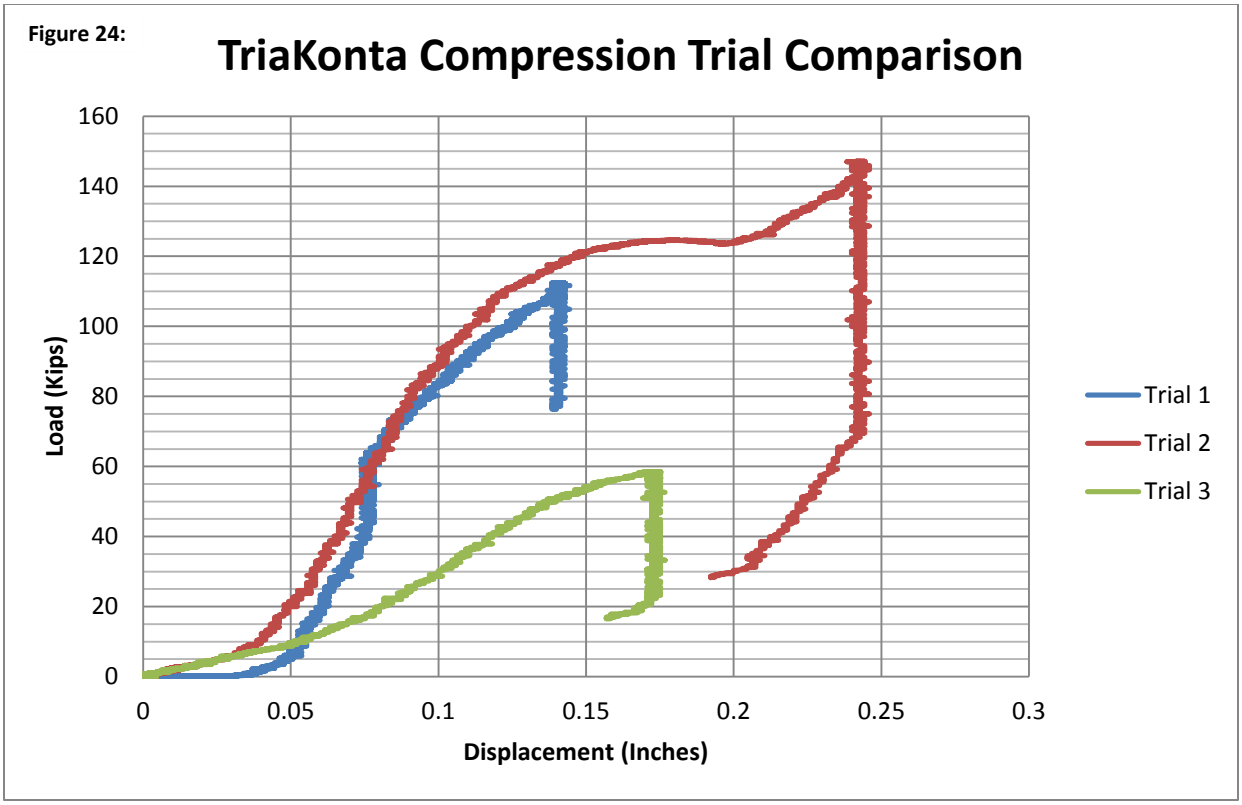

When looking at the tensile loading condition, the three samples performed consistently, with the maximum loading capacity falling between 55,000-65,000 lbs before failure (Figure 25). Displacement behavior was also consistent across the three samples throughout loading, with near indistinguishable displacement rates between the first and third trials, at ~1.2 inches before failure, and only a slightly increased but consistent displacement of ~1.4 inches during trial 2. The most common failure mechanisms under tensile loading was shear failure of the wooden struts at the exterior cross-pin to the strut face and splitting failure from the face through the same exterior cross-pins. Minor crushing was also observed at most cross pins. Despite failure of the wooden strut at the exterior cross-pins, the majority of damage to the interior pin and sleeve components were seen with the pins furthest from the ends of the struts, with moderate to significant bending deformation of these cross pins seen in all samples.

Figure 25:

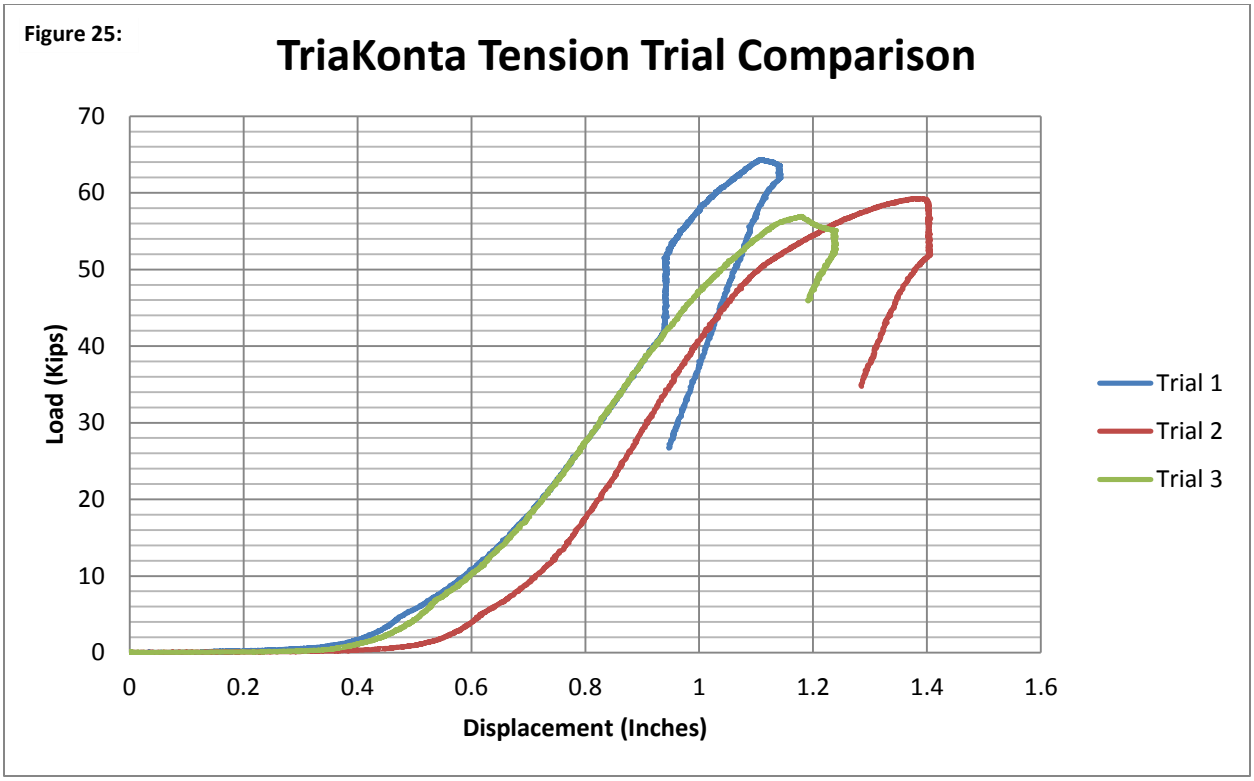

When looking at the bending loading condition (Figure 26) the three samples performed consistently throughout loading with a maximum loading capacity between ~16,000-18,000 lbs before failure. The reduction in applied load and increases in displacement can be seen at the failure points of the first and third trial where sudden and substantially splitting failure released a portion of the applied stresses. The second trial underwent a more gradual failure as seen in the slow flattening of the load/displacement curve. Splitting from the strut face through the exterior cross-pins in parallel with the load plane was the most common primary failure mechanism in the samples. Unlike the compression and tension load cases all structural damage to the connection assembly was isolated to the wooden struts in all bending samples.

Figure 26:

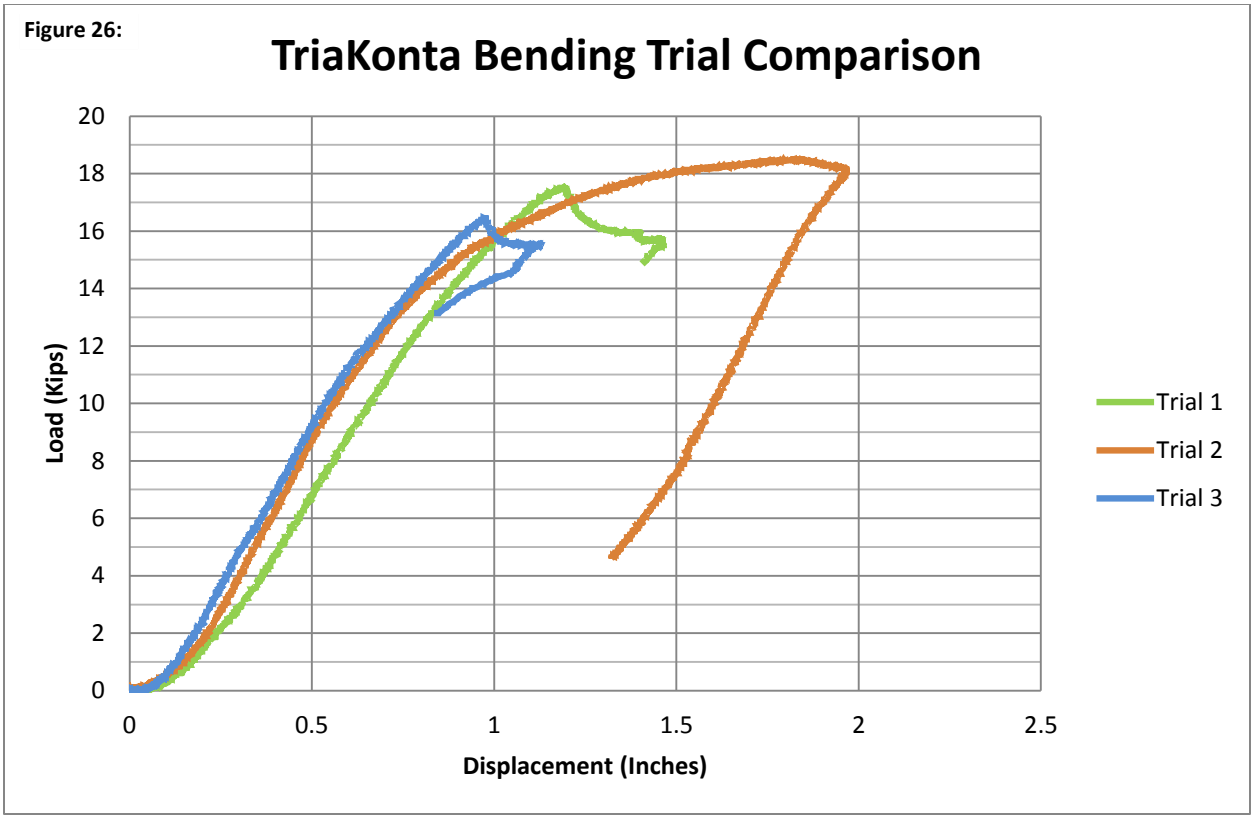
TriaKonta Bending Trial Comparison
Load (Kips)
20
18
16
14
12
10
8
6
4
2
0
0
0.5
1
1.5
2
2.5
Displacement (Inches)
Trial 1
Trial 2
Trial 3

Individual Trial Results:

Compression: Trial 1

Maximum Sustained Load:
112.3483 kips (499.7499 KN)

Maximum Displacement:
.144519 in (.367078 cm)

Description:

During our first compression test the sample was slowly taken to a maximum sustained load of approximately 112,000 lbs (Figure 27). The decision was made to discontinue increased loading for fear of damaging the node and cone prototypes. Longitudinal cracking in the strut sample began at approximately 35,000 lbs compressive load, with further cracking appearing at approximately 40,000 lbs compressive load (Figure 28). No additional cracking was observed for the remainder of sample loading. Post-test observation indicated that the cracking originated at the end of the struts, passing along the taper approximately 18” into the sample length. The load path seemed to be through the strut face, placing minimal stress on internal sleeve and pin components.

Figure 27:

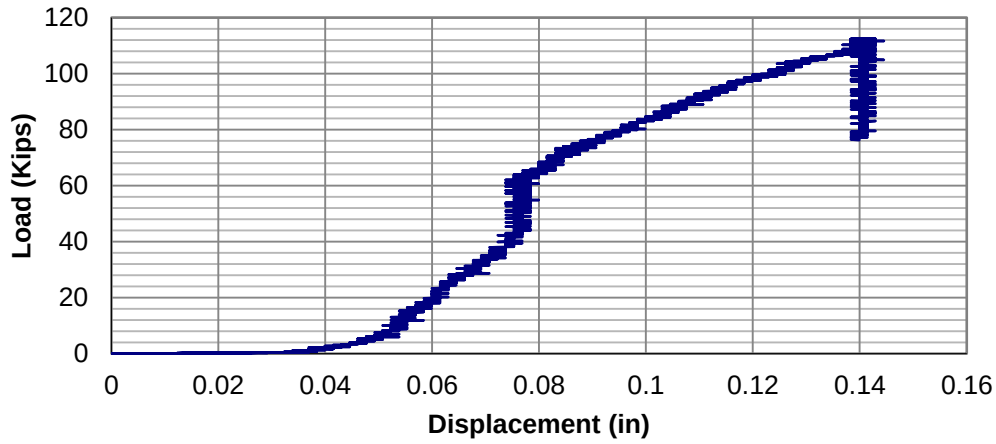

Figure 28: Longitudinal cracking at strut face.

Compression: Trial 2

Maximum Applied Load:
147.1038 kips (654.35008 KN)

Observed Failure Load:
~120 kips (533.8 KN)

Maximum Displacement:
.24599 in (.64281 cm)

Description:

Our second compression test took the sample to failure (Figure 29). As stated previously, our working assumption was the failure of the wooden components before steel. This assumption was proven to be incorrect. The second sample was taken to a maximum loading of approximately 147,000 lbs compressive load before yield failure in the node and cone were noticed and the test discontinued (Figure 30 & 31). Analysis of the video and test data showed preliminary yield failure of these sections at approximately 120,000 lbs compressive load. No significant cracks or damage to the wooden section of the strut during or after the test. Post-test observation showed

uneven crushing at the interface between the node face and cone, as well as bending deformation in the connective bolt. As mentioned earlier, this deformation was the result of the misalignments of the top and bottom nodes in the test jig. Repairs were made to the affected node and cone, and the damaged bolt was replaced for future testing.

Figure 29:

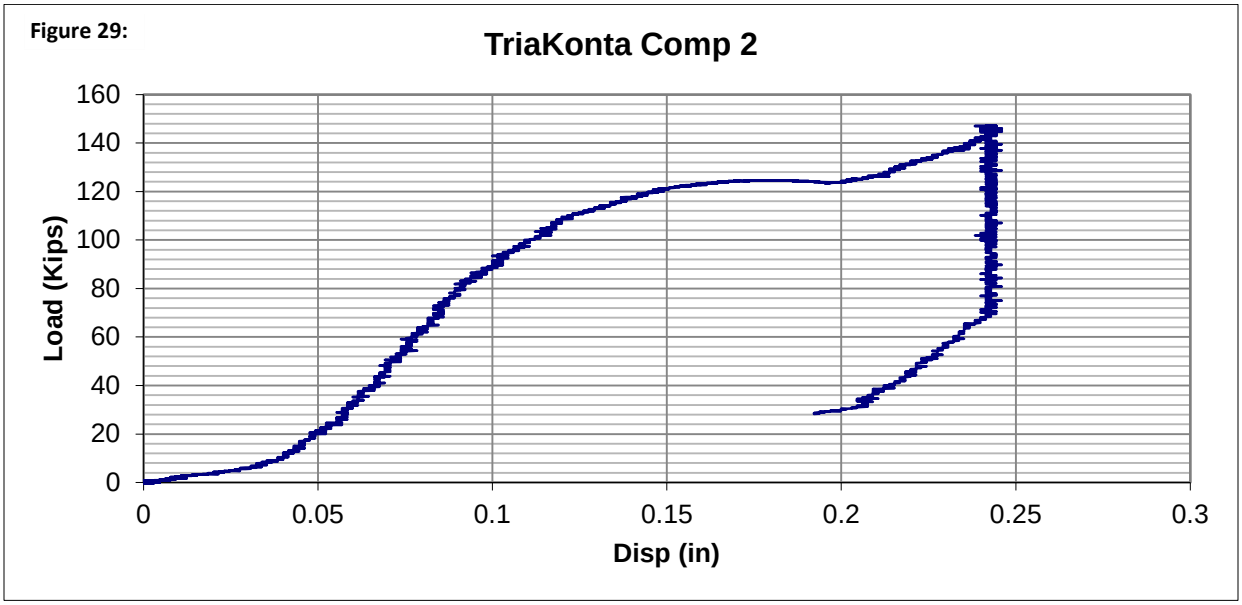

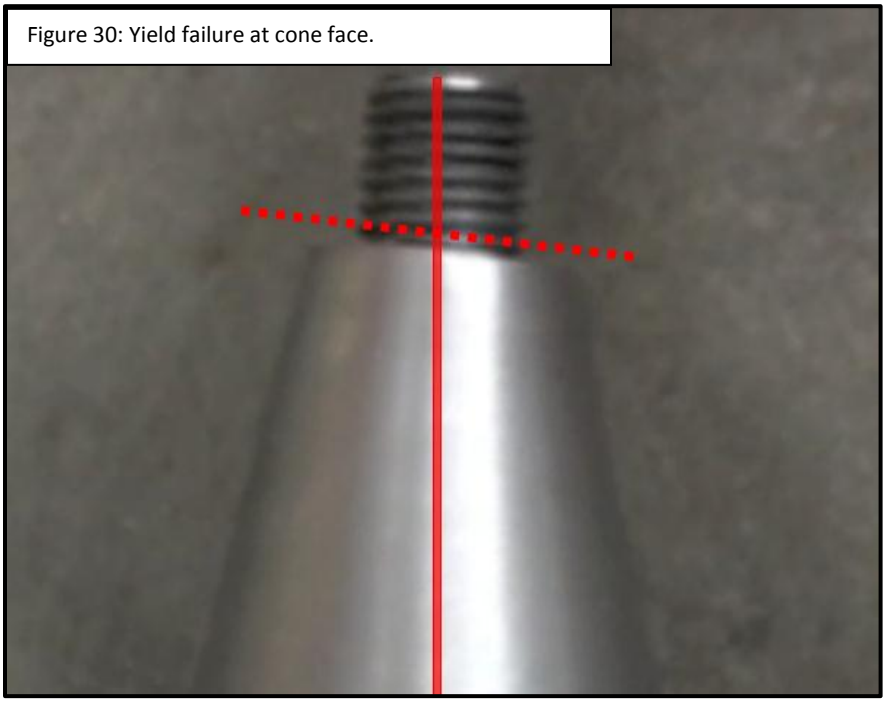

Figure 31: Yield failure at node face.

Compression: Trial 3

Maximum Applied Load:
58.51543 kips (260.2896 KN)

Maximum Displacement:
.176805 in (.44908 cm)

Description:

During our final compression test the sample was slowly taken to a maximum applied load of approximately 58,000 lbs (Figure 32). At this time the decision was made to discontinue increased loading due to preliminary yield failure at the interface of the steel cone and node. During the set-up of the third compression trial minor warping was observed along the length of the wooden strut. Restriction on lab time precluded the creation of a replacement sample and the warping prevented a fully centered placement of the node face against the testing apparatus (Figure 33). The loading on the sample was discontinued before noticeable damage could occur and post-test observation of the sample revealed no damage to the wooden strut or the steel components of the connection assembly.

Figure 32:

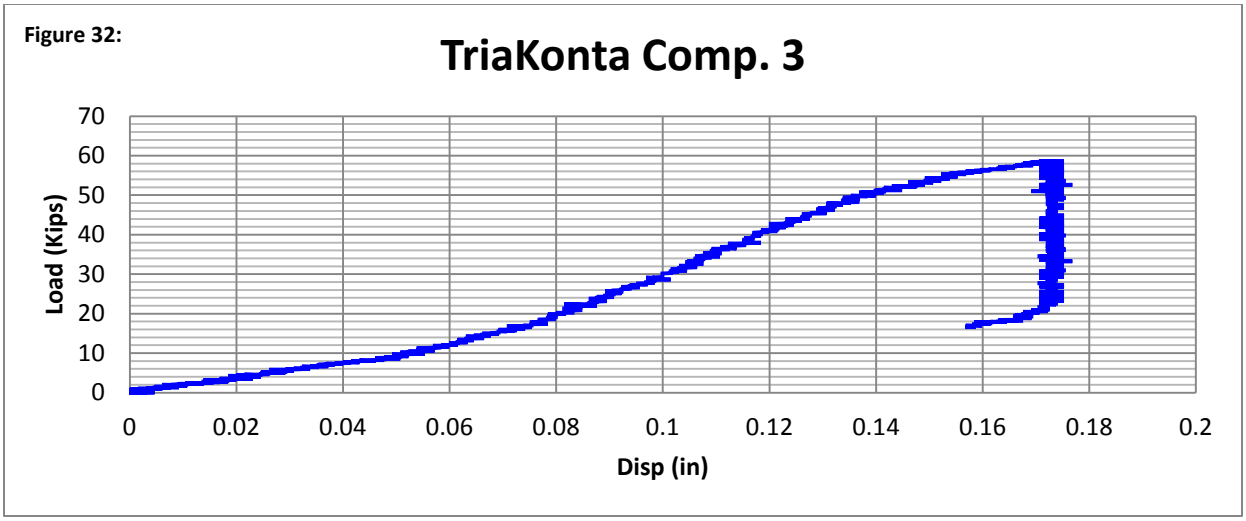

Figure 33: Off-center placement at compression plate.

Tension: Trial 1

Maximum Applied Load:
64.32535 kips (286.1334 KN)

Maximum Displacement:
1.143854 in (2.90539 cm)

Description:

During our first tension test the sample was loaded until failure, which occurred at approximately 64,000 lbs of tensile load (Figure 34). Additional minor cracking was observed during loading at approximately 52,000 lbs of tensile load. The primary failure mechanism was a shear failure of the wooden strut at a cross pin nearest the top end of the piece (Figure 35). Post-test observation and analysis showed small but uniform bending damage to all four cross pins, and related crushing damage around the pin holes in the wooden strut (Figure 36). The bolt itself appeared undamaged. However, the attachment sleeve suffered minor deformation, temporarily preventing the free rotation of the bolt within the sleeve assembly.

Figure 34:

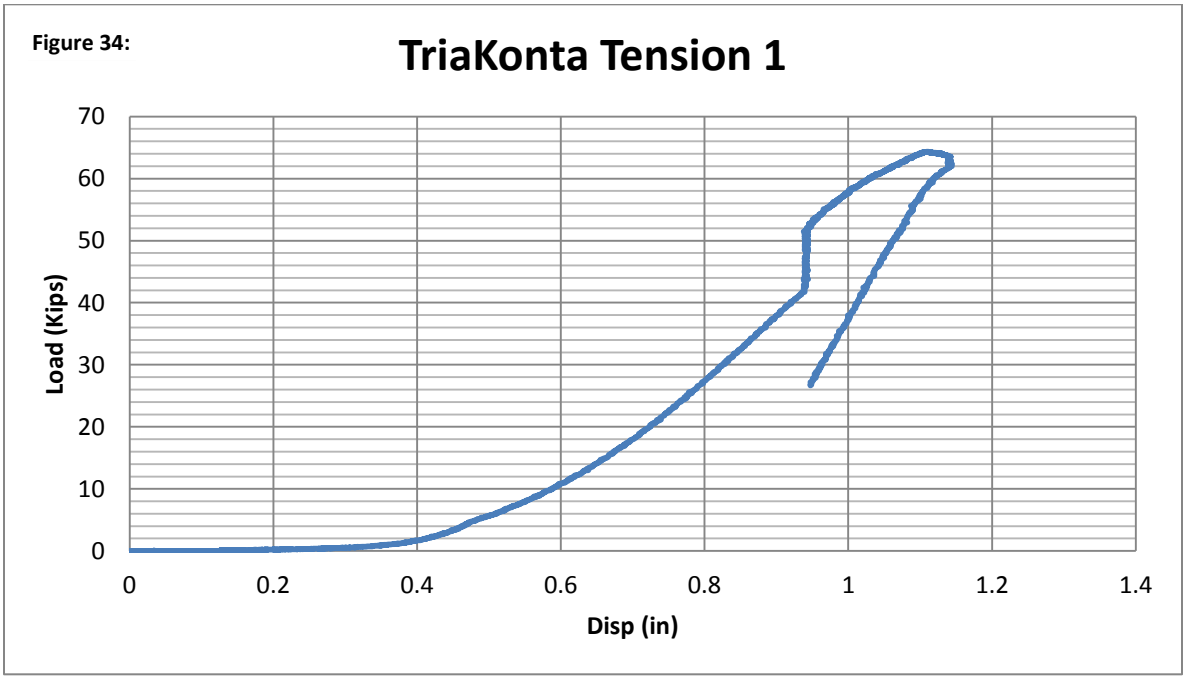

Figure 35: Shear failure of strut under tension.

Figure 36: Bending damage to steel cross pin.

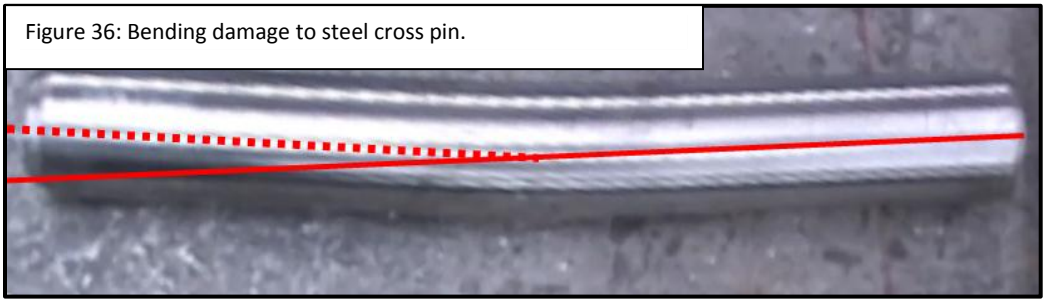

Tension: Trial 2

Maximum Applied Load:
59.2611 kips (263.6068 KN)

Maximum Displacement:
1.406755 in (3.57316 cm)

Description:

During the second tension test the sample was loaded to failure, which occurred at approximately 59,000 lbs of tensile load (Figure 37). Preliminary cracking first appeared at ~42,000 lbs of tensile load. Cracking continued uniformly through loading from this point until failure. The primary failure mechanism was a splitting failure at the

base of the sample created by movement of the bottom cross-pin closest to the strut face, with an additional shear failure at the cross-pin nearest the top face (Figure 38). Post-test observation and analysis showed significant bending deformation of the cross-pins closest to the center of the wooden strut with only minor bending deformation in the cross-pins nearest to the strut face (Figure 39). Related crushing damage was visible around the pin holes of the wooden strut. The bolt itself appeared undamaged; however the attachment sleeve suffered minor deformation temporarily preventing the free rotation of the bolt within the sleeve assembly.

Figure 37:

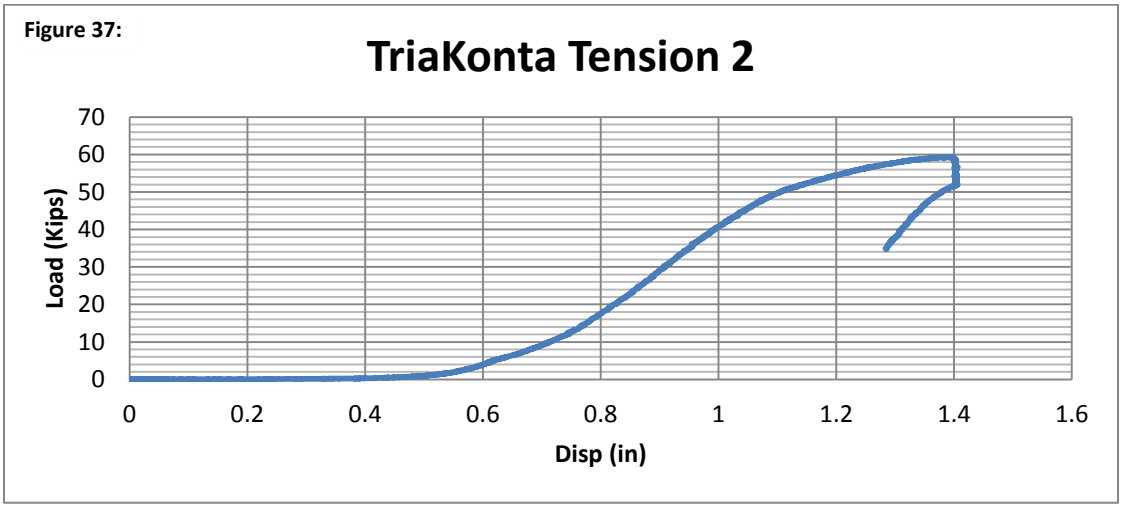

Figure 38: Splitting failure of strut under tension.

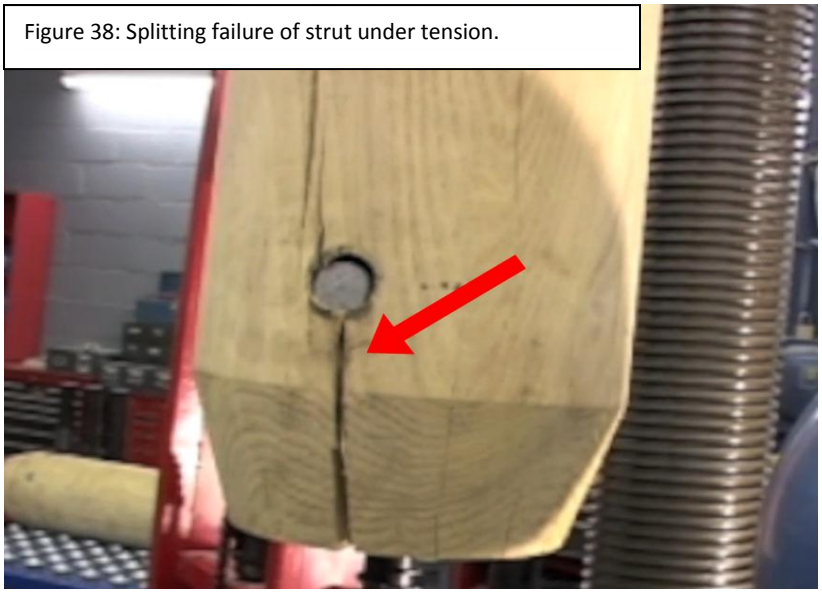

Figure 39: Bending damage to steel cross pin.

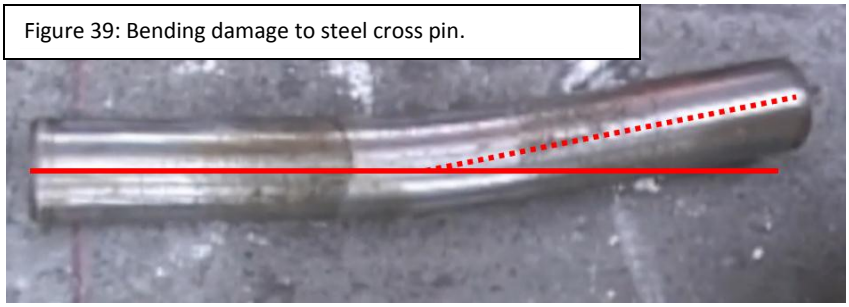

Tension: Trial 3

Maximum Load:
56.90252 kips (253.115 KN)

Maximum Displacement:
1.240712 in (3.15141 cm)

Description:

During the third tension test the sample was loaded to failure, which occurred at approximately 57,000 lbs of tensile load (Figure 40). Preliminary cracking first appeared at approximately 52,000 lbs of tensile load. Cracking continued rapidly as load increased until failure. The primary failure mechanism was a shear failure at the top of the sample created by movement of the top cross-pin closest to the strut face (Figure 41). In this sample, a single strip of screw tightened steel strapping was affixed around the wooden member near the member face to determine if such a measure would discourage cracking. The steel strapping additionally fractured at the moment of failure and was thrown from the sample having no observable impact of sample performance. There was no other significant failure in the sample. Post-test observation and analysis showed significant bending deformation of the cross-pin closest to the center of the wooden strut within the top connection with only minor bending deformation in other cross-pins (Figure 42). No significant crushing damage was visible around the pin holes of the wooden strut. The bolt and sleeve mechanism both appeared undamaged and were fully functional after extraction from the sample strut.

Figure 40:

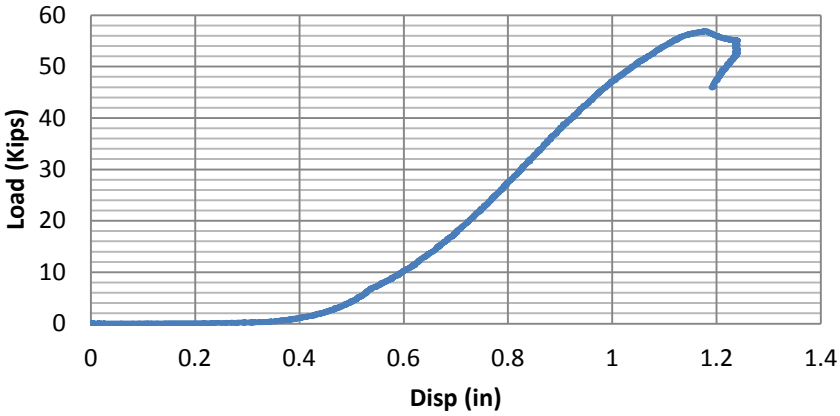

Figure 41: Shear failure of strut under tension.

Figure 42: Bending damage to steel cross pin.

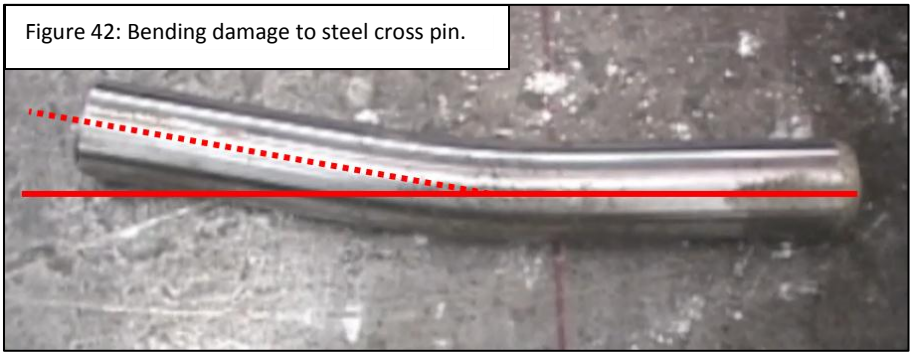

Bending: Trial 1

Maximum Applied Load:
17.5685 kips (78.1486 KN)

Maximum Displacement:
.144519 in (.367078 cm)

Description:

During the first bending test the sample was loaded until failure, which occurred at approximately 17,500 lbs of bending load (Figure 43). Preliminary cracking was observed intermittently during loading at approximately 5,000 lbs and 11,000 lbs of bending load. The primary failure mechanism was a splitting failure running parallel to the load plane from the face of the wooden strut and through the cross-pin closest to the face (Figure 44). During loading the position of the cone shifted relative to the strut face and compressed the strut face along the top half of the beam. Post-test observation and analysis showed no visible damage to the metallic components of the assembly with all mechanical failure isolated to the wooden strut.

Figure 43:

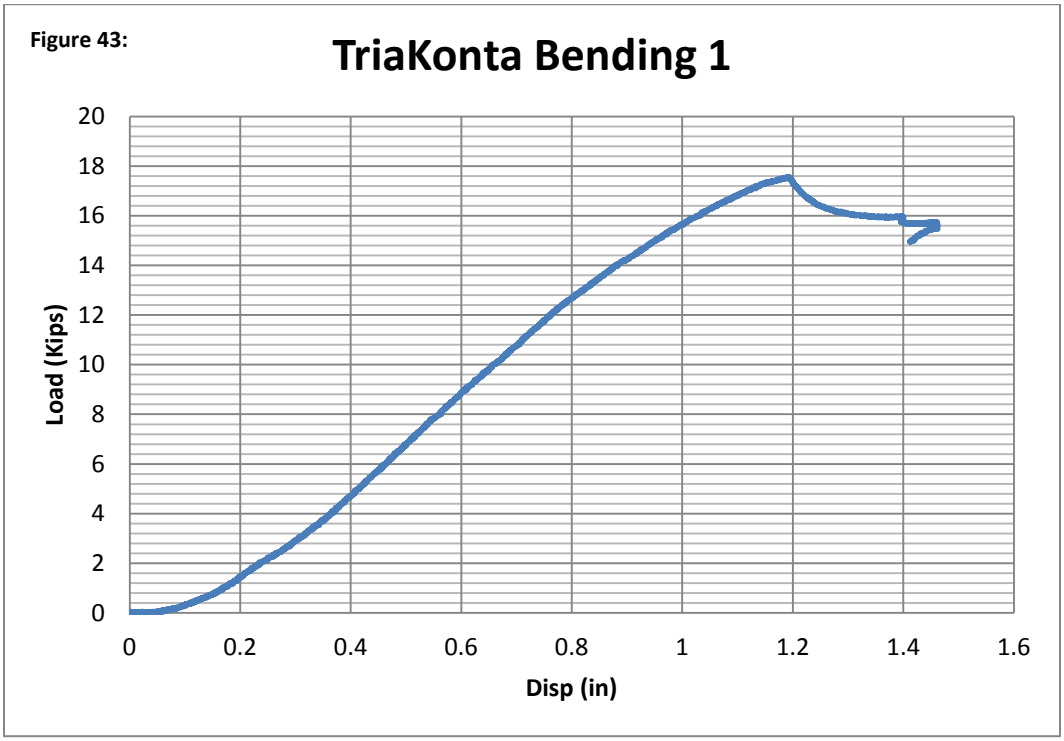

Figure 44: Splitting failure of strut under bending.

Bending: Trial 2

Maximum Load:
18.52237 kips (82.3159 KN)

Maximum Displacement:
1.451348 in (3.68642 cm)

Description:

During the second bending test the sample was loaded until failure, which occurred at approximately 17,500 lbs of bending load (Figure 45). Intermittent cracking was observed during loading, beginning at approximately 8,500 lbs of bending load. The primary failure mechanism of the sample was a splitting failure running near parallel to the load plane from the face of the wooden strut and partially through the cross-pin closest to the face (Figure 46). During loading the position of the cone shifted relative to the strut face and compressed the strut face along the top half of the beam. Post-test observation and analysis showed no visible damage to the metallic components of the assembly with all mechanical failure isolated to the wooden strut.

Figure 45:

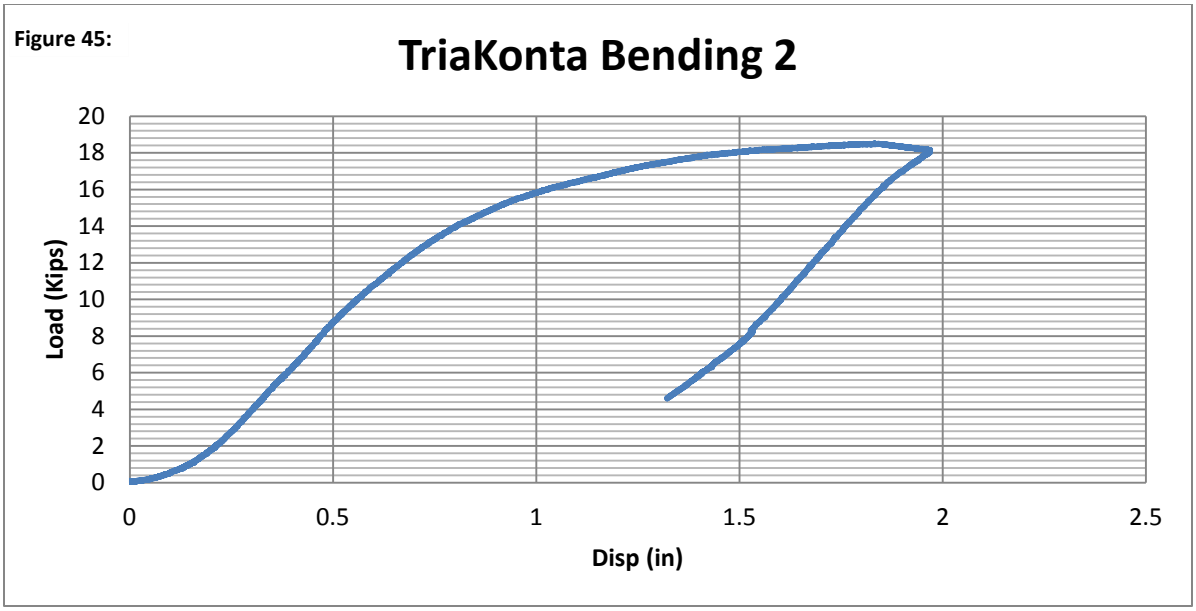

Figure 46: Splitting failure of strut under bending.

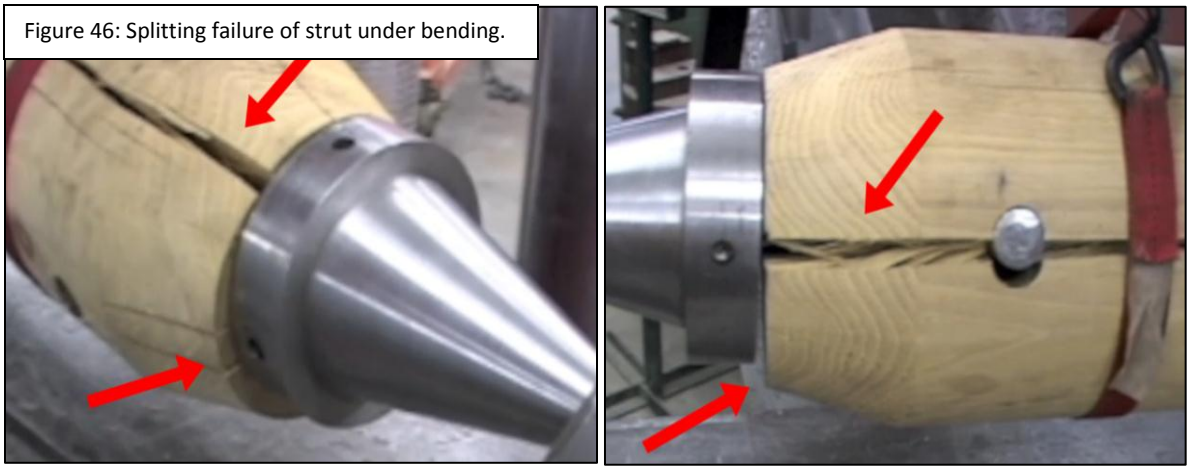

Bending: Trial 3

Maximum Load:
16.4585 kips (73.2113 KN)

Maximum Displacement:
1.126948 in (2.86245 cm)

Description:

During the third bending test the sample was loaded until failure, which occurred at approximately 16,500 lbs of bending load (Figure 47). Intermittent cracking was observed during loading, beginning at approximately 8,500 lbs of bending load. The primary failure mechanism of the sample was multiple splitting failures running at offset

axis to the load plane, running from the face of the wooden strut and through the cross-pin closest to the face (Figure 48). During loading the position of the cone shifted only slightly relative to the strut face and primary failure occurred before the cone was pulled away from the strut face. Post-test observation and analysis showed no visible damage to the metallic components of the assembly with all mechanical failure isolated to the wooden strut.

Figure 47:

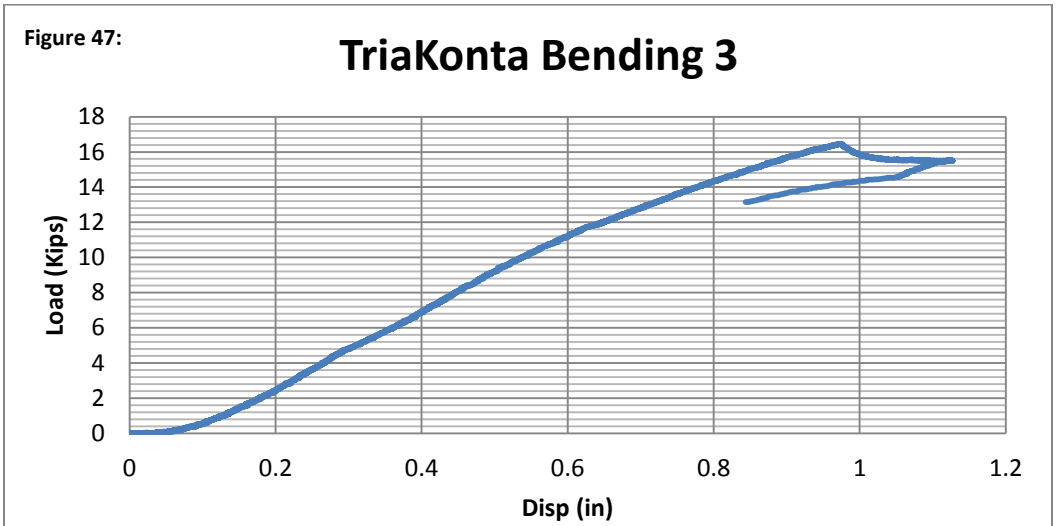

Figure 48: Cracking failure of strut under bending.

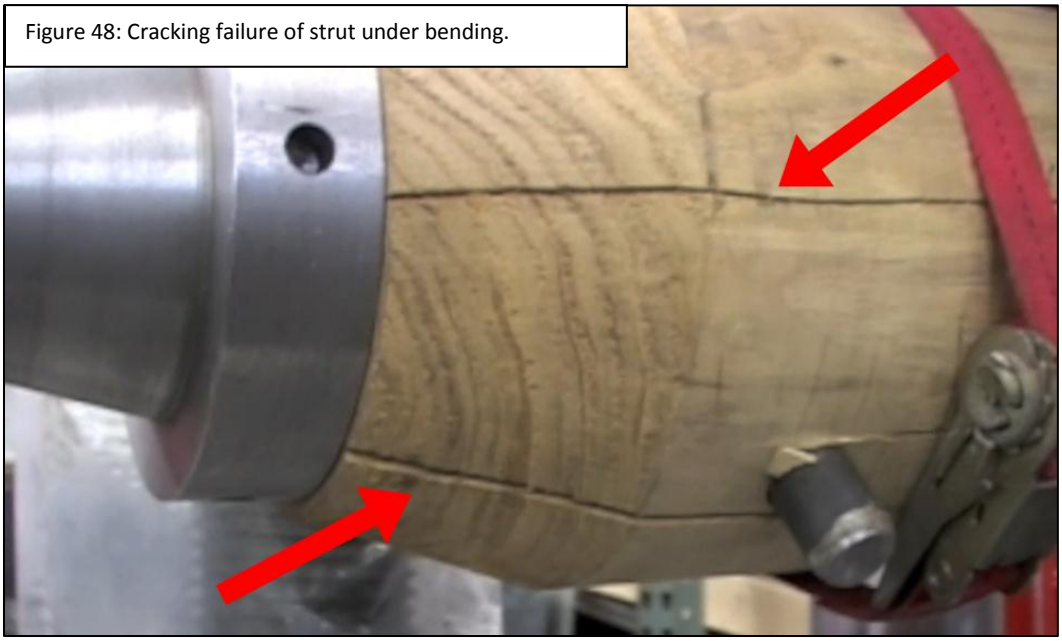

Discussion:

Viability of the Triakonta System

The final results from our proof of concept prototype trials support the viability of the Triakonta system, using black locust, in structural applications. While Black Locust as a wood species is not explicitly listed in the U.S National Design Standard for Wood Construction published by the American Wood Council, the comparable albeit weaker American hardwoods, Red Oak and Red Maple, can be used for rough comparison. The reference design values for visually graded timbers greater than 5"x5" for these species show the viability of the Triakonta system under real world structural stresses.

Table 3: Reference Design Values for Visually Graded Timbers (American Wood Council, 2005)

Design Values in lbs/in^2	Tension: (Parallel to Grain)	Compression: (Parallel to Grain)
Red Maple		
Select Structural Beams and Stringers	875 lbs/in^2	900 lbs/in^2
Red Oak		
Select Structural Beams and Stringers	850 lbs/in^2	875 lbs/in^2
Triakonta System (Black Locust)		
Triakonta Connection Members	~1094* lbs/in^2	~1990* lbs/in^2

*Values calculated using approximate maximum sustained loading values without failure, and cross sectional area of the strut.

Limitations of the Current Research

Despite the general success of the Triakonta system in structural testing, more research into the structural properties of system will be required before real world use. One of the primary limitations to this stage of research was the number of samples tested. Due to the significant variation in the mechanical properties of wood samples in general, the ability to test only three prototypical samples under each load condition is a significant barrier to drawing high confidence generalized conclusions about the performance of the system. Three unusually clear and homogenous wood samples in one of the loading conditions, particularly tension or bending, may have led to a higher

perceived performance than would be seen with a larger and more representative collection, in terms of composition and grade, of the locust wood samples. This same limitation applies to the metallic components of the system as well. Limitations in production capacity and resources required the reuse of every metallic component across samples and load conditions. This ended up being particularly significant with the invalidation of our primary testing assumptions, the failure of the strut before the metallic components, in the axial compression load condition. In order to more accurately test the system, dedicated components for the bolt assembly of each sample should be utilized, and compression testing should be conducted last if node and cone components are to be reused.

A second limitation in the research was the number of possible loading conditions tested. The Triakonta system is intended for use in space frames and shell structures and the demand forces experienced by the members is these kinds of structures are highly dependent on numerous factors, such as morphology, scaling, and the design and integration of non-structural building components, such as the façade and building equipment. The constraints of this research prevented a more comprehensive investigation of these possible demand forces, resulting in the possible exclusion of important test cases from this preliminary investigation.

Design Implications and Areas for Future Research

The performance of the Triakonta system under real world loading presented some possible opportunities for refinement of the design and areas of inquiry for further development of the system. The first and most significant possibility for the refinement of the design is in the number and geometry of the cross dowel pins. One of the most

surprising results of our testing was the significant bending damage caused to the cross dowel pins before strut failure during tension trials. One possible method of increasing the performance of the system in this area might be to increase the total number of pins while simultaneously reducing their diameter. This would allow the bearing stresses on the strut, applied by each of the cross pins securing the sleeve assembly, to be distributed across a greater area and a larger total bearing surface under loading, additionally reducing the bending stresses on the pins themselves. This strategy would more closely resemble a radially distributed multi-shear dowel joint, and would add minimal complexity to the production process.

A second area of inquiry for the refinement of the dowel pins would be to test alternative geometries for the pin cross section. One example would be the use of a rectangular pin with its longer side oriented in parallel with the load direct. While this kind of pin would be more resistant to bending under axial tension, further testing would be required to determine any additional effects to splitting and bearing potential this change in geometry might cause. This kind of change however may detrimentally affect ease of production as simple drilling would no longer be viable for creation of the pin holes.

A third possibility for the fastening of the sleeve assembly to the strut would be to eliminate the dowel pins altogether, adopting a process similar to the Cowley connector, using a chemical adhesive such as epoxy to secure the sleeve assembly within the wooden strut. The benefit of such a system would be the substantial simplification of production through the elimination of all materials, drilling and reaming associated with each dowel pin. This design, however, would essentially be irreversible, eliminating the

possibility of full disassembly and significantly reducing recycling potential at the end of the service life of the components. A second problem associated with this design would be the potential to introduce toxic chemistries associated with industrial adhesives to the system, many of which are known to be harmful to human health. That being said, newer less toxic alternatives are beginning to become available and may minimize this risk.

A fourth possibility to simplify production and to potentially reduce splitting in bending would be to use only the one cross dowel placed furthest from the end. In bending, the presence of a dowel pin created a weak zone in the wood, precipitating a cracking action, even if not aligned with the load plane. Additionally, this design modification may improve the performance of the system in tension since the failures were largely shear-based, rather than splitting. Such a design may result in increased bearing forces onto the single pin, but improving the bending strength of the steel is simply a matter of specification.

The final area of inquiry for refinement of the design would be in the geometry of the cone/node interface itself. Contrary to our original assumptions, the primary point of failure during axial compression was deformation and yield failure of the cone and node at their point of contact. A preliminary idealized calculation of the critical buckling load of a Triakonta long member with fixed pin connections and no lateral support show the strut capable of bearing far greater loads than seen during our compression test cases (Figure 49).

$$P_{cr} = \frac{\pi^2 EI}{{L_e}^2} \rightarrow P_{cr} = \frac{(3.14)^2(2.045x10^6\ psi)(\frac{\pi(4\ in)^4}{4})}{(.5(152\ in)^2} = 702{,}601\ \text{lbs}$$

Figure 49: Idealized buckling capacity of a fixed pin Triakonta long member.

If the circular cross section of the cone interface was replaced with a near hexagonal cross section, approximating the profile of the rhombic node face, and tapered to a cylinder at the strut, the contact area between the cone and node could be increased by more than 10%, allowing greater load distribution at the cone/node interface, increasing load potential without compromising geometric flexibility (Figure 50). If implemented however, care would be required during assembly to ensure alignment, and the complexity of the cone production would be increased.

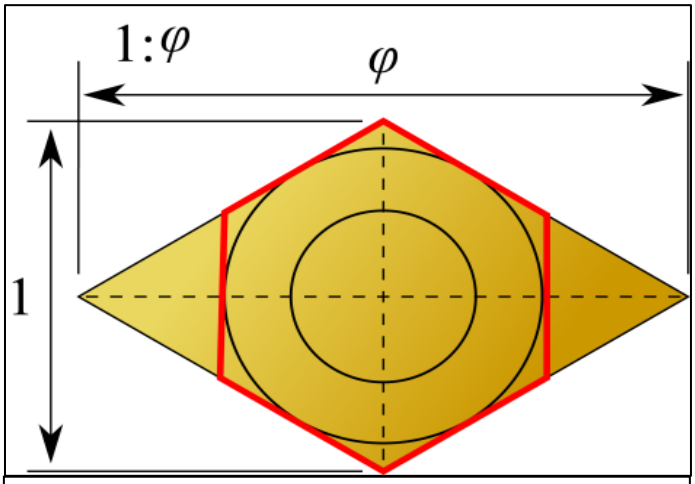

Figure 50: Hexagonal section profile for the cone/node interface.

Conclusions

The final results of our tests indicate that the Triakonta system is a potentially viable structural framing system. While these preliminary proof-of-concept tests are promising, broader and more comprehensive research and testing needs to be done for

these and additional loading conditions to suitably prove the reliability of the system before real world application.

The Triakonta system is unique in design and capability when compared to other systems available on the marketplace. While the system itself might be more geometrically and morphologically limited than framing and connection systems such as the Cowley Connector, which allow for high levels of customization, the Triakonta system and its reversible and deconstructable design makes it significantly better suited for mass production and the replacement of parts if failure should occur. The standardized component design additionally facilitates both assembly and disassembly and reuse at the beginning and end of the products useful life. As no single component is unique, the system can be interchangeably used throughout the superstructure of one or many building using the system.

In the end the Triakonta system provides an ecologically conscious and responsible structural model which provides a high degree of flexibility and visual order, while reducing the energy, carbon and material requirements of the built environment. It has the potential to change how we as designers and occupants view the lifecycle of a structure, and help to address the environmental challenges moving forward, we, who work with the built environment will surely face.

References

1) Addis, W. (2007). Building: 3000 years of design engineering and construction. London: Phaidon Press.
2) American Wood Council. *ANSI/AF&PA NDS-2005 National Design Specification (NDS) for Wood Construction, Table 4D: Reference Design Values for Visually Graded Timbers (5"x5" and larger),* American Wood Council (2005), p.48
3) Barrett, R.P., T. Mebrahtu, and J.W. Hanover. 1990. Black locust: A multi-purpose tree species for temperate climates. p. 278-283. In: J. Janick and J.E. Simon (eds.), Advances in new crops. Timber Press, Portland, OR.
4) Birdsey, R.A.; Lewis, G.M. 2003. 0. Gen. Tech. Rep. NE-310. Newtown Square, PA: U.S. Department of Agriculture, Forest Service, Northeastern Research Station. 42 p.
5) Bohl, R. W. (2001). Metallurgy for the non-metallurgist. *Metals: A History*. Materials Park, OH: ASM International, Materials Engineering Institute.
6) Buchanan, A. H. and S. B. Levine. 1999. "Wood-based Building Material and Atmospheric Carbon Emissions," Environmental Science & Policy 2: 427-437.
7) Burns, Russell M., and Barbara H. Honkala, tech. coords. 1990. Silvics of North America: 1. Conifers; 2. Hardwoods. Agriculture Handbook 654. U.S. Department of Agriculture, Forest Service, Washington, DC. vol.2, 877 p.
8) CIB, International Council for Research and Innovation in Building Construction. Publication 252, Overview of Deconstruction in Selected Countries. University of Florida Center for Construction and the Environment (August 2000)
9) Connectors for Construction. (2011).*Simpson Strong-Tie UK*. Retrieved August 25, 2011, from http://www.strongtie.co.uk/products/type.php?typeID=70&familyID=8
10) Cowley, G. (2011). Cowley Connectors. *Cowley Timberworks*. Retrieved August 7, 2011, from www.cowleytimberwork.co.uk/connectors.html
11) Crowther, P. (September, 1999). Design for Disassembly to Recover Embodied Energy. Unpublished paper presented at The 16th International Conference on Passive and Low Energy Architecture, Melbourne-Brisbane-Cairns, Australia.
12) Dispenza, K. (2011). Zaha Hadid's Heydar Aliyev Cultural Centre: Turning a Vision into Reality - Buildipedia.com. *Buildipedia - Latest Stories - Buildipedia.com*. Retrieved October 25, 2011, from http://buildipedia.com/on-site/from-the-job-site/zaha-hadids-heydar-aliyev-cultural-centre-turning-a-vision-into-reality
13) Elliott, J. (2010). *The Triakonta Structural Systems: From Toy to Tower,* Unpublished manuscript, Cornell University, Ithaca, NY

14) Gao, W., Ariyama, T., Ojima, T., & Meier, A. (2001). Energy impacts of recycling disassembly material in residential buildings. Energy and Buildings, 1(33), 553-562.
15) Geodesic Domes. (2011).*Minnesota Custom Mold Making Prototype Design Company*. Retrieved August 14, 2011, from http://www.oldmoldy.com/Geodesic_Domes.php
16) Glover, J., White, D., & Langrish, T. (2002). Wood versus Concrete and Steel in House Construction. Journal of Forestry, 100(8), 34-41.
17) Green, D., Winandy, J., & Kretschmann, D. (1999). Chapter 4: Mechanical Properties of Wood. *Wood Handbook—Wood as an Engineering Material* (pp. 1-45). Madison, WI: USDA Forest Products Labortatory.
18) Hargittai, I. (1992). *Fivefold symmetry* . Singapore: World Scientific.
19) Harris, C. (n.d.). Split-Ring Connector. *Dictionary of Architecture and Construction*. Retrieved August 15, 2011, from http://www.answers.com/topic/split-ring-connector-1
20) Lippke, B.; Wilson, J.; Perez-Garcia, J.; Bowyer, J.; Meil, J.2004. CORRIM: life-cycle environmental performance ofrenewable building materials. Forest Products Journal. 54(6): 13. (June 2004).
21) McLaren, W. (2009, July 2). Monsters in Our Midst. Amazing Magnified Images : TreeHugger. *TreeHugger*. Retrieved August 14, 2011, from http://www.treehugger.com/files/2009/07/monsters-in-our-midst-mazing-magnified-images.php
22) Navier biography. (n.d.). *MacTutor History of Mathematics*. Retrieved August 15, 2011, from http://www-history.mcs.st-andrews.ac.uk/Biographies/Navier.html
23) Negra, C.; Sweedo, C.; Cavender-Bares, K.; O'Malley, R.2008. Indicators of carbon storage in U.S. ecosystems: baseline for terrestrial carbon accounting. Journal of Environmental Quality. 37: 1376–1382
24) Nicholson, P., & Shaw, I. (2000). Wood: Procurement and Primary Processing. Ancient Egyptian Materials and Technology (pp. 353-368). Cambridge, UK: Cambridge University Press.
25) Niklas, K. (1997). Mechanical Properties of Black Locust (Robinia pseudoacacia L.) Wood. Sizeand Age-dependent Variations in Sap- and Heartwood. *Annals of Botany*,*79*(3), 265-272.
26) Orthotropic Material. (n.d.).*Solidworks Help*. Retrieved June 25, 2011, from help.solidworks.com/2010/English/SolidWorks/cosmosxpresshelp/AllContent/SolidWorks/NonCore/SimulationXpress/c_Orthotropic_Material.html

27) Pollet, C., Jourez, B., & Hebert, J. (2008). Natural durability of black locust (Robinia Pseudoacacia L.) wood grown in Wallonia, Belgium. *Canadian Journal of Forest Research*,*38*(6), 1366-1372.

28) *Timber joints - simple joints for frame construction. (n.d.). diydata.com do it yourself information and advice. Retrieved August 15, 2011, from http://diydata.com/techniques/timber_joints.php*

29) Schodek, D. L., & Bechthold, M. (2008). Structures (6th ed.). Upper Saddle River, N.J.: Pearson/Prentice Hall.

30) Steurer, A. (2006).*Developments in timber engineering: the Swiss contribution*. Basel: Birkhäuser.

31) U.S. Department of Agriculture Forestry Service. *American Woods FS-244, Black locust (Robinia Pseudoacacia L.),* U.S. Government Printing Office (1971)

32) U.S. Environmental Protection Agency. (2009). "Estimating 2003 Building Related Construction and Demolition Materials Amounts." Construction & Demolition Materials. U.S Environmental Protection Agency, n.d. Web. 10 Dec. 2011. http://www.epa.gov/osw/conserve/rrr/imr/cdm/pubs/cd-meas.pdf

33) White, Christopher. (2005) *Observations on the Development of Wood Screws in North America*. Museum of Fine Arts: Boston.